OXFORD
SOT | Society of Toxicology
www.toxsci.oxfordjournals.org

TOXICOLOGICAL SCIENCES, 148(2), 2015, 380–399

doi: 10.1093/toxsci/kfv205
Advance Access Publication Date: September 22, 2015
Research Article

2.45 GHz Microwave Radiation Impairs Learning and Spatial Memory via Oxidative/Nitrosative Stress Induced p53-Dependent/Independent Hippocampal Apoptosis: Molecular Basis and Underlying Mechanism

Saba Shahin,* Somanshu Banerjee,* Surya Pal Singh,† and Chandra Mohini Chaturvedi*,[1]

*Department of Zoology, Banaras Hindu University, Varanasi 221005, India and †Department of Electronics Engineering, Indian Institute of Technology (Banaras Hindu University), Varanasi 221005, India

[1]To whom correspondence should be addressed at Molecular Neuroendocrinology Lab, Department of Zoology, Banaras Hindu University, Varanasi 221005, India. E-mail: cmcbhu@gmail.com.

ABSTRACT

A close association between microwave (MW) radiation exposure and neurobehavioral disorders has been postulated but the direct effects of MW radiation on central nervous system still remains contradictory. This study was performed to understand the effect of short (15 days) and long-term (30 and 60 days) low-level MW radiation exposure on hippocampus with special reference to spatial learning and memory and its underlying mechanism in Swiss strain male mice, *Mus musculus*. Twelve-weeks old mice were exposed to 2.45 GHz MW radiation (continuous-wave [CW] with overall average power density of 0.0248 mW/cm^2 and overall average whole body specific absorption rate value of 0.0146 W/Kg) for 2 h/day over a period of 15, 30, and 60 days). Spatial learning and memory was monitored by Morris Water Maze. We have checked the alterations in hippocampal oxidative/nitrosative stress, neuronal morphology, and expression of pro-apoptotic proteins (p53 and Bax), inactive executioner Caspase- (pro-Caspase-3), and uncleaved Poly (ADP-ribose) polymerase-1 in the hippocampal subfield neuronal and nonneuronal cells (DG, CA1, CA2, and CA3). We observed that, short-term as well as long-term 2.45 GHz MW radiation exposure increases the oxidative/nitrosative stress leading to enhanced apoptosis in hippocampal subfield neuronal and nonneuronal cells. Present findings also suggest that learning and spatial memory deficit which increases with the increased duration of MW exposure ($15 < 30 < 60$ days) is correlated with a decrease in hippocampal subfield neuronal arborization and dendritic spines. These findings led us to conclude that exposure to CW MW radiation leads to oxidative/nitrosative stress induced p53-dependent/independent activation of hippocampal neuronal and nonneuronal apoptosis associated with spatial memory loss.

Key words: microwave radiation; hippocampal apoptosis; learning and spatial memory; oxidative and nitrosative stress; neurocytoarchitecture

Microwaves (MWs) are part of the electromagnetic spectrum with frequency ranging from 0.3 to 300 GHz and wavelength from 1 mm to 1 m. MW radiation, categorized as non-ionizing electromagnetic radiation (EMR), is absorbed at molecular level and induces nonthermal or thermal effects in vibrational energy or heating of the molecules. EMRs are classified as possible carcinogen (group 2B) for humans by International Agency for Research on Cancer (IARC). People heavily exposed to MW radiations are highly prone to nonmalignant tumors, acoustic neuromas, and malignant gliomas (Hardell *et al.*, 2003). To recommend exposure limits for safe uses International Council for non-ionizing Radiation Protection (ICNIRP) and the Institute

© The Author 2015. Published by Oxford University Press on behalf of the Society of Toxicology.
All rights reserved. For Permissions, please e-mail: journals.permissions@oup.com

of Electrical and Electronics Engineers (IEEE, 2005) have published guidelines, legislations, and recommendations about a decade back concerning the levels of exposure for the general public and workers due to health concern issues (IEEE Topical Review). MW radiation affects brain physiology as well as brain function in rodents and human. Continuous-wave (CW) and pulsed wave MWs (2.45 GHz, specific absorption rate [SAR] 6.8–100 W/kg) and mobile phone radiation severely affect the neuronal activity as well as results in neuronal apoptosis *in vivo* and *in vitro* (Joubert *et al.*, 2008; McRee and Wachtel, 1980; Salford *et al.*, 2003).

Number of studies demonstrated that CW as well as pulse field 2.45 GHz MW radiation results in cognitive malfunction and spatial working and reference memory deficits (Lai *et al.*, 1994; Wang and Lai, 2000). MW radiation affects the cultured hippocampal neuronal cell morphology and reduces excitatory synapses as well as the accuracy in working memory tasks (Odaci *et al.*, 2008; Xu *et al.*, 2006). In contrary, Cassel and other groups reported that whole body exposure to 2.45 GHz MW radiation does not affect/alter the radial maze performance as well as learning and memory (Cassel *et al.*, 2004; Cosquer *et al.*, 2005).

MW radiation acts as one of the strongest environmental stressor, inducing oxidative/nitrosative stress, caused by the excessive production of free radicals (Yakymenko *et al.*, 2015). Enhanced productions of reactive oxygen/nitrogen species (ROS/RNS) weaken the endogenous defense mechanisms and damage the cellular constituents including proteins, lipids, and nucleic acids (Ansari *et al.*, 2006). In the brain, such imbalance in ROS/RNS homeostasis can lead to neuronal damage (Bressler *et al.*, 2007).

Brain is highly sensitive to stress-induced neurodegeneration because of its high content of polyunsaturated fatty acids (PUFAs), which are vulnerable to free radical attacks and subsequently undergo lipid peroxidation (LPO) (Butterfield *et al.*, 2002). The antioxidant systems (enzymatic and/or non-enzymatic) scavenge the free radicals (ROS/RNS) and protect brain against oxidative/nitrosative damage (Ozturk *et al.*, 2005).

p53, a tumor suppressor and short-lived protein, elicits cellular response to a variety of stress signals (Riley *et al.*, 2008). Normally it is maintained at low levels, but DNA damage induced stabilization and accumulation of this protein in nucleus, induce or repress the transcription of cell-cycle progression genes (Sakaguchi *et al.*, 1998). Low level of p53 favors cell-cycle arrest so that DNA repair can occur, while a high level of p53 triggers apoptosis when repair seems to be impossible (Laptenko and Prives, 2006). Poly (ADP-ribose) polymerase (PARP-1), a nuclear DNA repairing enzyme, considered as an important apoptotic marker as being cleaved by active Capase-3 during apoptosis (Kaufmann *et al.*, 1993). High p53 alters Bcl-2/Bax ratio by suppressing the Bcl-2 and activating Bax and thus triggers Caspase-3 activation (Bivik *et al.*, 2006). Cleaved Caspase-3 as a key protease cleaves full length PARP-1 and results in apoptosis (Tewari *et al.*, 1995).

Energy homeostasis in brain may be disturbed due to the inactivation of Creatine kinase (CK)/loss in CK activity (via oxidation of its critical thiol) induced by ROS-mediated oxidative damage/oxidative stress (Aksenov *et al.*, 2000). Impairment of CK function plays an important role in the neurodegenerative pathway that leads to brain damage (Wendt *et al.*, 2002).

A considerable amount of research although with some contradiction has been focused on the behavioral impairments in rodents and in particular learning and memory deficits, following EMR exposure which might interfere with cognitive processes (Chaturvedi *et al.*, 2011; Li *et al.*, 2012). However, the underlying mechanisms of MW-induced learning disabilities and memory loss is still not well understood. Our aim is to highlight the MW irradiation induced neuronal structural/anatomical alterations in different hippocampal subfields (DG, CA3, CA2, and CA1) to offer mechanistic insights into the spatial memory based operations (MWM) performed by the exposed rodent hippocampus. We hypothesized that short- and long-term low level 2.45 GHz (CW) MW irradiation impairs learning and spatial memory in mice via oxidative and nitrosative stress induced p53-dependent/independent hippocampal neuronal and nonneuronal apoptosis. To test this hypothesis, we have checked the alterations in (1) learning and spatial memory, (2) area/region specific hippocampal neuronal cytoarchitecture, (3) hippocampal oxidative and nitrosative stress, and (4) area/region specific expression of pro-apoptotic proteins (p53 and Bax) and inactive executioner Caspase-3 (pro-Caspase-3) and full length/uncleaved PARP-1 in hippocampus. These pro-apoptotic and apoptotic factors together in combination play a crucial role in the execution of apoptosis.

In this study, we elucidate the mechanistic pathways through which low level 2.45 GHz MW radiation triggers the hippocampal neuronal and nonneuronal cell death via inducing oxidative/nitrosative stress and leads to subsequent loss in learning and spatial memory.

MATERIALS AND METHODS

Study Design

Swiss strain male mice (12 weeks old, body weight approximately 30 grams) were obtained from the mice colony of our laboratory maintained under light:dark cycle (LD12:12). Animals were kept under steady state, received standard commercial pelleted food and water *ad libitum*. Randomly selected, 40 mice were divided into 4 groups (1 sham control and 3 experimental, ie, 15 days exposed; 30 days exposed and 60 days exposed group) of 10 mice each ($N = 10$). Experimental group mice were exposed to 2.45 GHz (CW) MW radiation for 2 h/day from 09:00 to 11:00 h (30 days), 11:30 to 13:30 h (60 days exposed and 60 days sham exposed) and 14:00–16:00 h (15 days) continuously. The control group mice were subjected to sham exposure for 60 days. Only 1 sham control of maximum duration, ie, 60 days sham exposed group was taken into account in this study to nullify the cage related and other external constraints as from our preliminary studies we have observed that the data of 15 and 30 days sham exposed as well as cage control animals/groups were not significantly different from those of 60 days sham exposed animals/groups. Rectal temperature of all the mice was monitored during the first and the last 3 days of exposure. Experiment was conducted in accordance with institutional practice and within the framework of the revised animals (Scientific procedures) act of 2002 of the Government of India on Animal welfare. This study is performed according to the regulation of "Institutional Animal Ethical Committee, Faculty of Science, Banaras Hindu University."

The experiment was repeated twice, hence the data presented is from total 20 animals per group including Morris water maze. Further, out of total 20 animals in each group, 5 animals (3 from study-1 and 2 from study-2) used for Golgi staining to study the cytoarchitectural and cytomorphometrical alterations in the neurons of area specified regions of hippocampus (viz. DG, CA1, CA2, and CA3), 5 animals (2 from study-1 and 3 from study-2) for immunohistochemistry of pro-apoptotic proteins (p53 and Bax), inactive executioner Caspase-3 (pro-Caspase-3),

and uncleaved/full-length DNA repair enzyme (PARP-1) to investigate the degree of apoptosis and rest 10 animals (5 from each study) were processed for biochemical estimations.

Exposure Setup

MW power to pyramidal horn antenna was delivered by the Analog Signal Generator MW source (Model no. E 8257D PSG, manufactured by Agilent Technologies). The experimental setup used for MW irradiation of mice consists of Analog Signal Generator covering a frequency range from 250 kHz to 20 GHz, a coaxial attenuator, MW amplifier (model no. 8349B Hewlett Packard Co), coaxial to waveguide transition, 20 dB cross coupler and E-plane bend, pyramidal horn antenna in addition to animal cage kept in a box covered by MW absorbers (Figure 1). Pyramidal horn antenna was made up of silver polished brass material. Its throat and mouth dimensions were 7.2×3.2 cm and 9.0×5.0 cm, respectively, and axial length of the antenna from the throat was 10.0 cm. Gain of the horn antenna (G_t) was found to be 4.0657 dB, as calculated by 3-antenna method. The distance between pyramidal horn and the mid plane of animal body (assuming the body length to remain horizontal during exposure) was estimated through far field criterion ($R \geq 2D^2/\lambda$) to be 25 cm (Figure 1). The animal cage cross-sectional dimensions in E and H-planes (electric and magnetic field planes, respectively) were designed on the basis of 1.24 and 1.69 dB beamwidths in corresponding planes of the horn, respectively. For this purpose, the horn radiation patterns were also measured at 2.45 GHz in E and H-planes (Chaturvedi *et al.*, 2011). Maximum output power measured by the power meter with power sensor (Model no. 836 A, manufactured by Agilent Technologies) was 19.8 dBm delivered to the horn antenna from the amplifier. The power meter has a range from 30 μW to 3 W (Model no. 8481H, Hewlett Packard Co).

Animal cage was designed in such a way that it contained 10 compartments of equal sizes. The dimension of the animal cage was $19.2 \times 17.6 \times 15$ cm and each compartment was $3.5 \times 8.5 \times 15$ cm accommodating single mouse at a time. Pine wood material with low dielectric constant was used for making the cage and its partitions. For air ventilation, small circular holes of 1 cm diameter were drilled on the side and the partition walls of the cage and the upper portion of the cage remained open. Base as well as sides and partition walls of the cage were covered by carbon impregnated Styrofoam MW absorber to reduce the reflections of scattered beam. Each mouse was kept in the separate compartment of the cage throughout the exposure period. The partitions were made in such a way that mice remain restrained in the cage during the period of MW irradiation and were exposed with their length parallel to E-field. The animal cage was placed on the stand in a box covered from all the 4 sides by MW absorbers to minimize reflections (Figure 1). Mice were exposed daily for 2 h. The temperature in the chamber was maintained at 25°C–27°C throughout the exposure period by circulating air. The 20 dB cross coupler and power meter with power sensor were used to measure the power input to antenna and reflections from it. Power transmitted from the antenna was equal to 64.776 mW and this was estimated by subtracting the power reflected from the antenna (when it faces toward free space), from the measured input power. The maximum power density (S_{max}) obtained at the center (on-axis) of the exposure cage kept in the far field region of the horn was computed by using the following formula:

$$Power\ Density = \frac{P_t\, G_t}{4\Pi R^2}$$

where P_t is the power transmitted into the cage, G_t is the gain of the horn and R is the distance between the horn aperture and mid plane of the body of mouse in the exposure cage. The maximum power density (S_{max}) obtained at the center (on-axis) is found to be 0.0289 mW/cm^2. The off-axis power density $S_{(\theta,\ \varphi)}$ within the space of exposure cage is less than S_{max} by a factor $F_{(\theta,\ \varphi)} < 1$ called the normalized radiation pattern.

The power density obtained close to the boundary of the cage in E-plane is found to be

$$F_{(\theta,\ \varphi)}|_{-1.24\text{dB points}} \times S_{max} = 0.752 \times 0.0289 = 0.0217\ \text{mW/cm}^2$$

Similarly, the power density close to the boundary of the cage in H-plane is

$$F_{(\theta,\ \varphi)}|_{-1.69\ \text{dB points}} \times S_{max} = 0.678 \times 0.0289 = 0.0196\ \text{mW/cm}^2$$

The power density obtained in other regions of the exposure cage is in between S_{max} (obtained at the center) and that

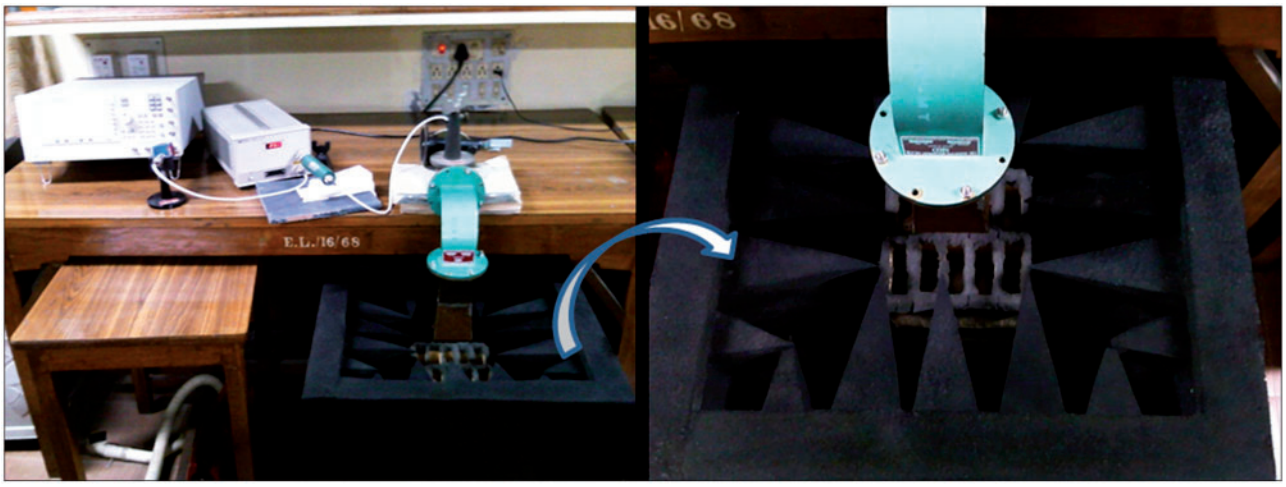

FIG. 1. Microwave (MW) exposure setup and the position of animal cages during MW exposure. Mice were exposed to low level 2.45 GHz continuous-wave (CW) MW radiation for 2 h/day continuously for 15, 30, and 60 days by using MW source and Pyramidal horn antenna (overall average Power density = 0.0248 mW/cm^2 and overall average whole body specific absorption rate value = 0.0146 W/Kg).

obtained close to cage boundary in E-/H-plane. Therefore, average power density within the space of cage in E-plane is 0.0253 mW/cm^2 while in H-plane the average value is 0.0243 mW/cm^2. The approximation for overall average power density obtained within the space of the exposure cage is

$$\frac{0.0253 + 0.0243}{2} = 0.0248\,\mathrm{mW/cm^2}$$

Because SAR is directly proportional to power density (Gandhi *et al.*, 1977) therefore, SAR values of 10 mice also vary according to the position of the mice within the exposure cage. The maximum average whole body SAR obtained for the mouse in the central region of the cage is 0.017 W/Kg.

The factors used to estimate the incident power density close to the boundaries in E- and H-planes can be employed to determine the average whole body SAR of the animals placed close to the boundaries in the 2 planes. Therefore, approximation for overall average whole body SAR of 10 mice can be computed to be 0.0146 W/Kg.

Mice of experimental group were exposed to 2.45 GHz MW radiation at overall average Power density of 0.0248 mW/cm^2 and overall average SAR value of 0.0146 W/Kg. The SAR value was estimated for body length parallel to the electric field, as per actual placement of the mouse (Gandhi *et al.*, 1977; Shahin *et al.*, 2013, 2014). The exposure at overall average power density of 0.0248 mW/cm^2 did not cause any elevation in the ambient temperature of animal cage as well as mice rectal temperature. The average observed rectal temperature of the mice were 35.81°C ± 0.2°C (control group) and 35.9°C ± 0.2°C (experimental group) during first 3 days of exposure and 35.91°C ± 0.2°C (control group) and 35.95°C ± 0.2°C (experimental group) after the end of exposure.

Morris Water Maze

Spatial learning and memory was assessed by using standard Morris (1984) water maze task as described previously. In brief, it consists of a circular pool tank (120 cm in diameter) filled with water in a suitably equipped room with a constant temperature of 22°C ± 1°C and humidity. For spatial learning in the acquisition (hidden-platform) test, mice were required to find the hidden platform using spatial cues available in the testing room. A translucent acrylic platform (10 cm in diameter) was located in the center of the northeast quadrant and submerged 1 cm below the water surface throughout training period. The mice were subjected to 4 trials per day over 5 consecutive days. The starting position for each trial was randomly chosen and counterbalanced across all of the experimental groups. In each of the 4 trials, the mouse was gently released into the water by facing the tank wall at 4 different starting positions equally spaced around the perimeter of the pool. The mouse was allowed to swim for a maximum of 60 s or until it located the submerged platform and was allowed to stand on the platform for 20 s. If a mouse did not find the platform within the time limit, it was led to it by hand and allowed to rest on it for 20 s. The time that an individual mouse took to reach the hidden platform was recorded as the escape latency for its spatial learning score. To assess the retention of spatial memory, a probe test was conducted 24 h after the last training trial, in which the hidden platform was removed. The mouse was released into the water from the opposite quadrant with respect to the target quadrant and allowed to swim freely for 60 s. The time spent by individual mouse in the target quadrant that previously contained the hidden platform was respectively recorded as a measure of spatial memory. Visible platform test (4 trials per day for 2 days) was used to ensure that impairments were not related to sensorimotor impairments or noncognitive factors (deficits of vision, motivation, or locomotor function). In this trial, the visible platform was positioned 1 cm above the water surface. The position of the cued platform was moved during each trial to reduce the animal's use of extramaze spatial cues in locating the platform. MWM test was performed under blind condition during the last 8 days of MW exposure. After the completion of each exposure, animals were transferred to laboratory cages and handed over to an experimenter (who did not know the exposure conditions) to perform the Morris water maze test.

Tissues Sampling

Twenty-four hour after the last day of MW exposure, mice were sacrificed by decapitation and brain was dissected out. Brain of 5 mice from each group was processed for Golgi staining and other 5 mice brain was fixed in 4% paraformaldehyde solution for Immunohistochemistry. Hippocampus was separated from other 10 mice brain and stored at −20°C after washing with ice-cold sterile physiological saline until processed for different biochemical assays.

Golgi Staining

Brain of mice was processed for rapid Golgi staining technique as described earlier (Shankaranarayana and Raju, 2004). In brief, brain were soaked in a solution containing 5% potassium-dichromate, 5% chloral hydrate, 8% glutaraldehyde, 6% formaldehyde, and 500 μl DMSO for 1 day at room temperature in the dark. This solution was then replaced by a fresh solution and incubation was continued for another 4 days. Tissues were then washed and transferred to a solution containing 0.75% $AgNO_3$. After 3–4 days, brain were removed, dehydrated in alcohol and then embedded in paraffin wax. Transverse sections (40 μm thick) of hippocampus were cut with a rotatory microtome (Leica). Sections collected serially were dehydrated with ascending series of alcohols, cleared in xylene, mounted on gelatin-coated slides, and cover slipped for inspection.

Analysis of Neuronal Morphology

Golgi stained sections of the brain were viewed under a microscope (Axioskop 2 Plus; Carl Zeiss AG, Oberkochen, Germany) and images were captured with a digital camera. Average soma diameter and axonal length (ie, the distance of axon from the soma to the point where the axon disappears either leaving the plane of section or by failure to impregnate further) of different neurons were determined in 10 sections per mouse brain ($N = 5$) by using the image analyzer software Motic Images 2000 version 1.3. The number of pyramidal neurons in CA1, CA2, and CA3 was counted by using a ×40 objective lens and Motic Images 2000 version 1.3 software.

Dendritic Spine Density

By using the Camera Lucida system (Carl Zeiss), all protrusions, irrespective of their morphological characteristics, were counted as spines if they were in direct continuity with the dendritic shaft (von Bohlen und Halbach *et al.*, 2006). For the purpose of this study, dendrites directly originating from cell soma were classified as primary dendrites, and those originating from primary dendrites were classified as secondary dendrites. Spine number was calculated by tracing the length of dendrite (at least ≥ 10 μm long). Starting from the origin of the branch, and continuing away from the cell soma, spines were counted along 10 μm stretch of the dendrite. The values for number of spines

from each 10 μm segment, at a given distance from the origin of the branch, were then averaged across all neurons.

Tissue Homogenization

For nitric oxide (NO) and ROS estimation, hippocampus were homogenized in 50 mM phosphate buffer (pH 7.4) for 30 s using a Polytron homogenizer and after adding protease inhibitor 0.2 μM PMSF, were centrifuged at 12,000 × g for 30 min at 4°C. The resultant supernatant was used for measuring malondialdehyde (MDA) level and determining antioxidant enzymes (superoxide dismutase [SOD], catalase [CAT], and glutathione peroxidase [GPx]) and creatine kinase (CK) activity. Total protein concentration was measured by Lowry's method using BSA as standard. For all the biochemical assays, the hippocampal samples were processed by experimenter under blind condition.

Total ROS Level

The total ROS generation in fresh homogenate of hippocampus was assessed by using the method of Bejma *et al.* (2000) with slight modification. For this, 2′7′-dichlorodihydrofluorescein diacetate (DCFH-DA), a nonpolar compound was used as a probe. DCFH-DA after conversion to a polar derivative by intracellular esterase can rapidly react with ROS to form the highly fluorescent compound dichlorofluorescein. Briefly, the homogenate was diluted in PBS to obtain a concentration of 25 μg tissue protein/ml. The reaction mixture containing diluted homogenate and 10 μl of DCFH-DA (10 μM) was incubated for 15 min at room temperature to allow the DCFH-DA to be incorporated into any membrane-bound vesicles and the diacetate group cleaved by esterase. After 30 min of further incubation, the conversion of DCFH-DA to the fluorescent product DCF was measured by using a spectrofluorimeter with excitation at 484 nm and emission at 530 nm. Background fluorescence (conversion of DCFH-DA in the absence of homogenate) was corrected by the inclusion of parallel blanks.

Estimation of Total Nitrite and Nitrate Concentration

NO, a reactive free radical is generally oxidized to NO_x (nitrite-NO_2^-/nitrate-NO_3^-). The total nitrite and nitrate concentration was measured by the indirect method of Sastry *et al.* (2002) in hippocampus by using acidic Griess reaction for color development after the reduction of nitrate with copper-cadmium alloy and deproteinization. In brief, the reaction mixture was prepared by adding 100 μl of sample or standard (KNO_3), 400 μl of carbonate buffer and a small amount (0.15 g) of activated copper-cadmium alloy fillings (washed in buffer and dried on a filter paper) in the tube. The reaction mixture was then incubated at room temperature for 1 h with thorough shaking. The reaction was stopped by the addition of 100 μl of 0.35 M sodium hydroxide (NaOH), followed by 400 μl of 120 mM zinc sulphate ($ZnSO_4$) solution under vortex and allowed to stand for 10 min. The tubes were then centrifuged at 8000 × g for 10 min. One hundred microliter aliquots of the clear supernatant were transferred into the wells of a microplate (in quadruplicate) and Griess reagent (50 μl of 1.0% sulphanilamide prepared in 2.5% orthophosphoric acid and 50 μl of 0.1% N-naphthylethylenediamine prepared in distilled water) was added to it with gentle mixing. After 10 min, the absorbance was measured at 545 nm against a blank (containing the same concentrations of ingredients but no biological sample) in a microplate reader (MS5605A, ECIL, Hyderabad, India) using the path check option.

LPO Assay

Level of lipid peroxides was measured by estimation of MDA, end product of LPO by the method of Ohkawa *et al.* (1979) with a slight modification. MDA reacts with thiobarbituric acid (TBA) to yield a colored compound. Briefly, to 100 μl of tissue homogenate, 50 μl of 0.8% butylated hydroxytoluene, 750 μl 0.8% of TBA, 750 μl of 20% acetic acid (pH 3.5), and 100 μl of 8% SDS were added. The reaction mixture was then incubated at 95°C in water bath for 1 h. After this, the mixture was cooled down by keeping on ice for 15 min and then centrifuged at 2000 × g for 10 min. Absorbance was taken at 532 nm and the results was expressed as nmoles MDA/mg protein.

Estimation of Total Carbonyl Groups

Duplicate aliquots of different MW irradiated group hippocampus homogenates (approximately 500 μg of protein) were treated with 10% (wt/vol) trichloroacetic acid (TCA) (Fagan *et al.*, 1999). Pellets were collected by high-speed centrifugation and suspended by probe sonication in 200 μl of 2 N HCl or 200 μl of 10 mM DNPH in 2 N HCl. After incubation for 1 h at room temperature, proteins were precipitated again with TCA. Removal of unreacted DNPH was carried out by washing the pellets once with 1 ml of 10% (wt/vol) TCA and thrice with 1 ml of ethanol:ethyl acetate (1:1 vol/vol). Proteins were dissolved by sonication in 1 ml of 100 mM Tris-HCl buffer, pH 7.5, containing 2% SDS. Insoluble material was removed by centrifugation. The absorbance of the supernatant of the HCl-treated sample was assessed at 360 nm and subtracted from that of the DNPH-treated sample. The amount of carbonyl groups was calculated by using a molar extinction coefficient of 22,000 cm^{-1} at 360 nm. It is noteworthy that this method is considered by many to be an indicator of total protein carbonylation (Levine *et al.*, 1994). However, DNPH also reacts with non-PCO-containing compounds, eg, nucleic acids; (Fagan *et al.*, 1999) that are both present in the tissue samples and precipitated with TCA. These values were considered to be a measure of total carbonyls (TCOs) rather than of protein carbonyl (PCO) (Cao and Cutler, 1995).

Antioxidant Enzymes

Superoxide dismutase. The total SOD activity in hippocampus was determined by the method of Das *et al.* (2000). The reaction mixture consisted of 100 μl of sample, 150 mM phosphate buffer (pH7.4), 20 mM L-methionine, 50 μM EDTA, 1% Triton X-100, 100 μM riboflavin and Greiss reagent. The absorbance was taken at 543 nm. The value of SOD was calculated in term of units defined as the amount of SOD that inhibits the reduction of nitroblue tetrazolium by 50%. The final results were expressed as unit of SOD per mg of protein.

Catalase. Catalase activity in the hippocampus in different group was assayed according to Aebi (1984). Briefly, the reaction mixture contained 1.9 ml of 50 mM phosphate buffer (pH 7.0) and appropriate dilution of tissue supernatant to make a volume 2 ml. Reaction was initiated by addition of 1 ml of freshly prepared 30 mmol H_2O_2 and the decrease in absorbance was measured at 240 nm for 2–3 min. One unit of CAT represents the decrease of 1 μM of H_2O_2 per minute. The molar extinction coefficient for H_2O_2 is 43.6 $M^{-1}cm^{-1}$.

Glutathione peroxidase assay. GPx activity was assayed as described by Mantha *et al.* (1993). The reaction mixture (1 ml) contained 50 μl sample, 398 μl of 50 mM phosphate buffer (pH 7.0), 2 μl of 1 mM EDTA, 10 μl of 1 mM sodium azide, 500 μl of

0.5 mM NADPH, 40 µl of 0.2 mM GSH and 1U glutathione reductase. The resultant mixture was allowed to equilibrate for 1 min at room temperature. After this, the reaction was initiated by addition of 100 mM H_2O_2. The absorbance measured kinetically at 340 nm for 3 min. The GPx activity was expressed as µmol of oxidized NADPH oxidized to $NADP^+$ per min per mg of protein using an extinction coefficient (6.22 $mM^{-1}cm^{-1}$) for NADPH.

Biochemical Estimation of Creatine Kinase (CK) Activity. CK activity was determined by the method of Zhuravliova *et al.* (2009). CK catalyzes the incorporation of phosphate into creatine to form creatine phosphate. The amount of phosphates existing in a free form as a result of ATP hydrolysis in the mitochondrion were evaluated in the form of the phosphovanadium-molybdate complex and analyzed spectrophotometrically. In brief, reaction medium contained 100 µl homogenate and 500 µl solution of creatine (1.9 mM) prepared in special buffer (2.5 mM glycine + 2 mM Na_2CO_3 + 0.2 mM $MgSO_4$, pH 9.7). The resulting mixture was suspended for 5 min at 37°C; then 500 µl of ATP (0.07 mM) was added and further incubation was performed at 37°C for 60 min. The enzyme reaction was stopped by adding 14% solution of TCA. The resulting solution was then centrifuged for 10 min at 3000 × g. Approximately 500 µl of supernatant was mixed with 500 µl of ammonia vanadate and ammonia molybdate mixture (1:1). The phosphate was assessed spectrophotometrically at 400 nm wavelength.

Immunohistochemistry of Full Length p53, Bax, Pro-Caspase-3, and Full Length/Uncleaved PARP-1

Immunohistochemistry for full length p53, Bax, pro-Caspase-3, and full length/uncleaved PARP-1 were carried out on paraformaldehyde-fixed paraffin-embedded brain sections using polyclonal antibodies. Antibodies with specificity to the full length p53 (sc 6243, FL-393), Bax (sc 6236), pro-Caspase-3 (sc 7148), and uncleaved PARP-1 (sc 8007) were from Santa Cruz Biotechnology (Santa Cruz). Immunohistochemistry was performed in a 2-step procedure by using Vectastain ABC kit (Vector Laboratories, Burlingame, California). In the first step, after initial deparafinization in xylene and rehydration in graded series of alcohol, slides were incubated with goat—full length p53 antisera (dilution 1:100), rabbit—Bax antisera (dilution 1:100), rabbit—pro-Caspase-3 antisera (dilution 1:100), and mouse—full length/uncleaved PARP-1 antisera (dilution 1:100) for 24 h in humid chamber, respectively (Shahin *et al.*, 2014). In second step, slides were incubated with horseradish peroxidase-conjugated goat anti-rabbit immunoglobulins for 30 min. Finally, diaminobenzidine hydrochloride was used as a chromogen molecule for the immunological detection.

Image Analysis

The total number of immunoreactive full length p53, Bax, pro-Caspase-3, and full length/uncleaved PARP-1 cell bodies in DG, CA1, CA2, and CA3 was counted automatically by using a × 40 objective lens and Motic Images 2000 version 1.3 software. The sections were divided into series, and just one of these was counted. Once images of these series containing immuno-positive cells were captured, background threshold levels were adjusted to allow for automatic counting of *ir*-neuronal and nonneuronal cells in these sections by the software package. In addition, the ImageJ software placed a dot on each cell counted, allowing the observer to verify accuracy during the counting process. On the basis of intensity of signals *ir*-cells were divided into intense, moderate, and weak *ir*-cells.

Statistical Analysis

Time-dependent/short-term and long-term MW radiation exposure induced changes in cognitive functions, hippocampal neuronal cell morphology and dendritic spine number, nonenzymatic, and enzymatic oxidative stress markers and quantitative analysis of IHC plate are reported as means ± SEM. For statistical analysis, 1-way ANOVA coupled with a Dunnet T3 *post hoc* analysis was used to determine the significance of various parameters among the 4 different groups. A P value of < 0.05 was considered significant. Data were statistically analyzed by using the SPSS software.

RESULTS

Time-Dependent 2.45 GHz (CW) MW Irradiation Results in Learning and Spatial Memory Deficits in Mice

Learning and spatial memory functions of all groups of mice were assessed by Morris water maze task. Analysis revealed that with increased duration of exposure, the rate of learning declined significantly. As compared with control, 15 days (day 1, 3–5, $P < .05$; day 2, $P < .01$), 30 days (day 1–3, 5, $P < .01$; day 4, $P < .001$), and 60 days (day 1–5, $P < .001$) 2.45 GHz (CW) MW exposed group exhibited slow learning and took more time to reach the platform (Figure 2A). Further analysis revealed a significant effect of 2.45 GHz (CW) MW irradiation on the escape latency over all training days in 15 days ($P < .05$, Figure 2B), 30 days ($P < .01$, Figure 2B), and 60 days ($P < .001$, Figure 2B) exposed group of mice, demonstrating significant difference in the escape latency over the 5 days of training period between the 3 groups, indicating that MW irradiated mice had impaired spatial learning function compared with sham control mice. Escape latency time (ELT) that is the time required to find the hidden platform increased significantly in MW irradiated group of mice compared with sham control. Moreover, ELT was significantly higher in 30 and 60 days exposed group of mice compared with 15 days exposed group over all the training days (Figure 2B), suggesting a chronic effect of long-term MW irradiation. The percentage of nonfinder also increased in all the exposed groups of mice compared with control and the percentage of nonfinder significantly increased in 30 ($P < .01$), and 60 days ($P < .01$) MW irradiated group compared with 15 days ($P < .05$) exposed mice (Figure 2C).

The spatial memory of all the 4 group mice was evaluated by the probe test performed after 24 h of the last training session. Unlike sham control, 2.45 GHz MW irradiated mice demonstrated impaired retention performance during probe trials. Specifically, they spent significantly less time in the target quadrant where the platform had been (Figure 2D) and crossed over the former platform location significantly fewer times than sham controls. This indicates impaired spatial memory retention in 2.45 GHz MW irradiated mice than sham control which showed significantly higher levels of retention during the probe trials in terms of target quadrant time. Moreover, 15 days exposed mice spent more time in the target quadrant than 30 and 60 days exposed mice but significantly less time than sham control, indicating that the CW long-term MW irradiation may lead to permanent memory impairment/deficit. In addition, the visible platform trials in the Morris water maze revealed no significant differences in escape latency, swimming speed, or swimming (data not shown). This implies that the memory impairments of 2.45 GHz MW irradiated mice were not due to visual or motor dysfunctions or motivational shortage. Taken together, 15, 30, and 60 days CW 2.45 GHz MW irradiated mice

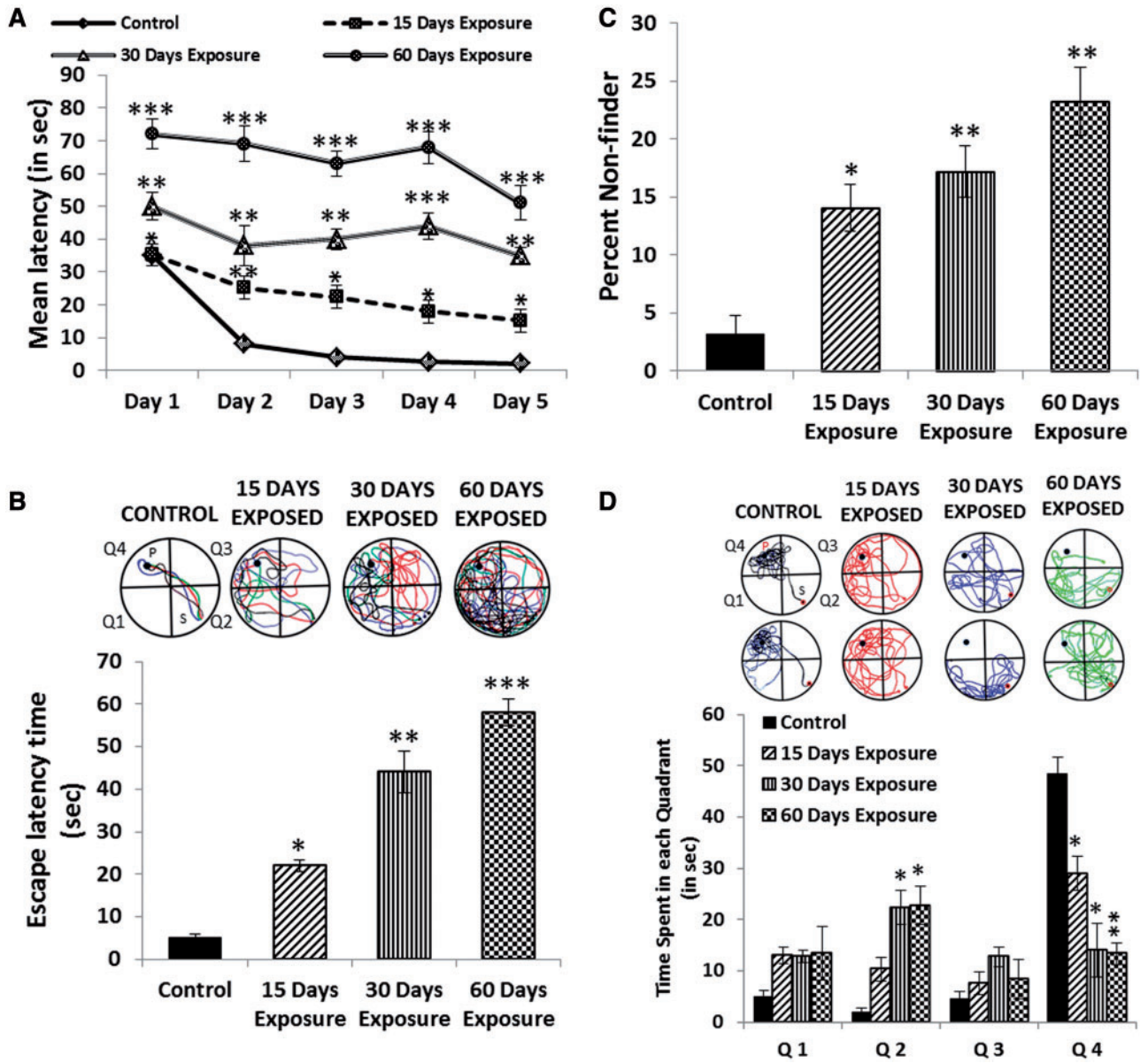

FIG. 2. Effect of 15, 30, and 60 days 2.45 GHz (CW) MW radiation on learning and spatial memory of Swiss albino mice. A, Spatial learning: Morris water maze performance during acquisition of animals received 5 days of training. Each point is the average latency to the target for 4 consecutive trials. Each day presents 4 trials. Water maze performance shows a significant increase in latency time on the first day of training. Learning was significantly reduced in all the exposed group of mice compared with sham control. B, Upper panel shows the swim path (Q-quadrant and P-platform) of 4 mice on the last day of training period and lower panel shows the escape latency time (ELT) of mice over the 5 days of training period during water maze test to locate the hidden platform. Note significant increase in ELT after 15, 30, and 60 days MW irradiation. Control group follows the shorter route or distance in minimum time to locate the hidden platform, 15 days exposed mice took long distance and seems to be confused while 30 days and 60 days exposed mice move randomly and take more time to locate the platform. C, Percent nonfinders: percentage of mice not able to find the platform increase in time-dependent manner after 2.45 GHz MW irradiation. D, Upper panel shows the search path (Q-quadrant and P-platform) and lower panel shows the time spent in each quadrant during the day of Probe trail. Note that MW-exposed mice showed a significant decrease in the time spent in Q-4 (target quadrant) during the last day (Probe trail) when platform was removed. Each value represents the mean ± SEM ($N = 20$). Significance of the difference was determined by using 1-way ANOVA. *$P < .05$, **$P < .01$, and ***$P < .001$ significance of difference from control.

showed marked hippocampus-dependent learning and spatial memory deficits in the water maze test.

CW 2.45 GHz MW Irradiation for Different Duration Causes an Extensive Decrease in Dendritic Arborization of Neuron and Spine Number

In this study, we examined the effects of short- and long-term CW 2.45 GHz MW irradiation on dendritic arborization of neuron and spine number in hippocampus region of brain which plays an important role in processing and remembering spatial information. We observed a significant decrease in the dendritic arborization of neuron in CA1, CA2, and CA3 region of hippocampus in all the 2.45 GHz MW irradiated group of mice (Figure 3A). The number of pyramidal neurons which is very important for memory formation decrease significantly in all the 2.45 GHz (CW) MW irradiated groups of mice compared with control. Moreover, in 60 days exposed group of mice no pyramidal neuron was observed in the different regions of hippocampus. The diameter of neuronal soma (pyramidal as well as other types of neurons) increased significantly while the axonal

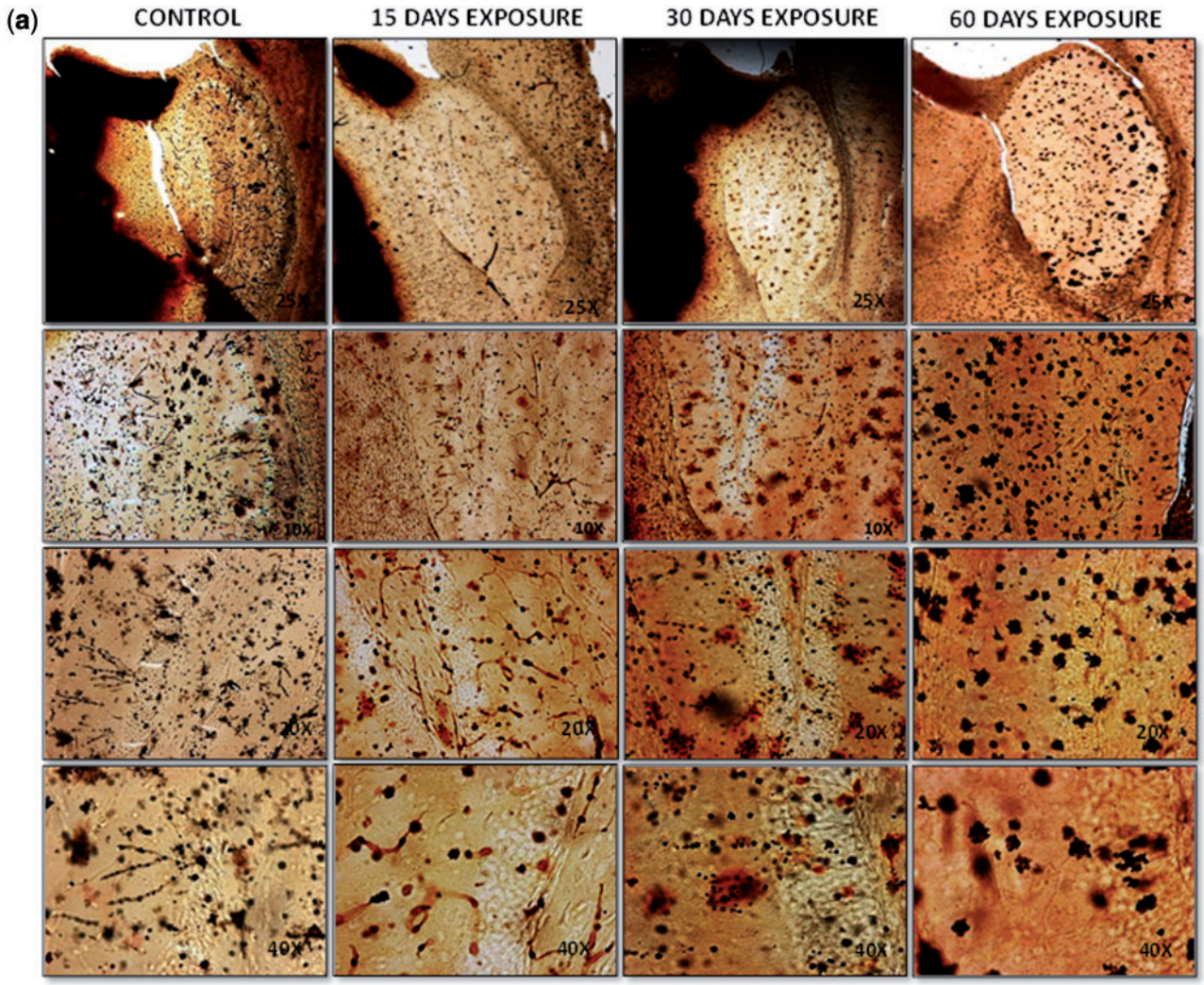

FIG. 3. A, Representative Golgi impregnated neurons in the hippocampus region of 15, 30, and 60 days 2.45 GHz (CW) MW irradiated mice. Note highly reduced number of neurons, neuronal and dendritic arborizations in CA1, CA2, CA3, and DG region of all the 2.45 GHz (CW) MW irradiated group of mice as compared with control. Number of dendritic spines also reduced after 15, 30, and 60 days MW exposure. Note increased neuronal clumping or clogging in mice received 30 and 60 days 2.45 GHz MW irradiation. B, Morphology of neurons present in the CA1, CA2, and CA3 region of hippocampus. Number of dendrites decrease significantly in time-dependent manner in all the exposed group of mice. Number of apoptotic or degenerating neurons increased in 30 and 60 days of 2.45 GHz (CW) MW exposed group of mice. Note neuronal clumping or clogging in 60 days 2.45 GHz (CW) MW irradiated mice. C, Number of spine per 10 μm decreased significantly in the CA1, CA2, and DG region of Hippocampus in MW exposed group of mice compared with control. Data were determined by using 1-way ANOVA. ***$P < .001$ significance of difference from control.

length decreased significantly in all the exposed group of mice compared with control (Table 1). These changes were more prominent in the hippocampal region of 30 and 60 days MW irradiated mice compared with 15 days exposed mice. This indicates a decreased in synaptic plasticity due to neuronal loss and reduced dendritic arborization in different region of hippocampus. Neuronal clogging was observed in 30 and 60 days MW irradiated group (Figure 3B). Next, we examine the effect of 2.45 GHz MW radiation on spine number. MW irradiated mice revealed a significant reduction in number of spine per 10 μm segment of dendrite for both primary and secondary branches compared with sham control ($P < .001$; Figure 3C).

CW 2.45 GHz MW Irradiation for Different Duration Causes Havoc Production/Overproduction of Free Radicals in Hippocampus

Brain tissue is particularly vulnerable to oxidative damage because of its high consumption of oxygen and the consequent generation of high quantities of free radical. Growing data suggest that injury resulting from oxidative stress may play an important role in the pathophysiology following acute neurological insults. As free radical and oxidative stress-induced neuronal cell death has been implicated in various neurological disorders and MW radiation is also responsible for generating oxidative stress, we examined ROS production in hippocampus region. Significant increase in ROS production compared with control was observed after 15 ($P < .05$), 30 ($P < .001$), and 60 days ($P < .001$) MW-irradiated animals (Figure 4A). Along with ROS, we have also checked the level of NO in different group after CW 2.45 GHz MW irradiation, as NO play an important role during chronic stress and apoptotic cell death in the hippocampus. The total nitrite and nitrate concentration which is an indirect measure of NO level was found to be significantly increased after 15 ($P < .05$), 30 ($P < .01$), and 60 days ($P < .001$) CW 2.45 GHz MW irradiation (Figure 4B).

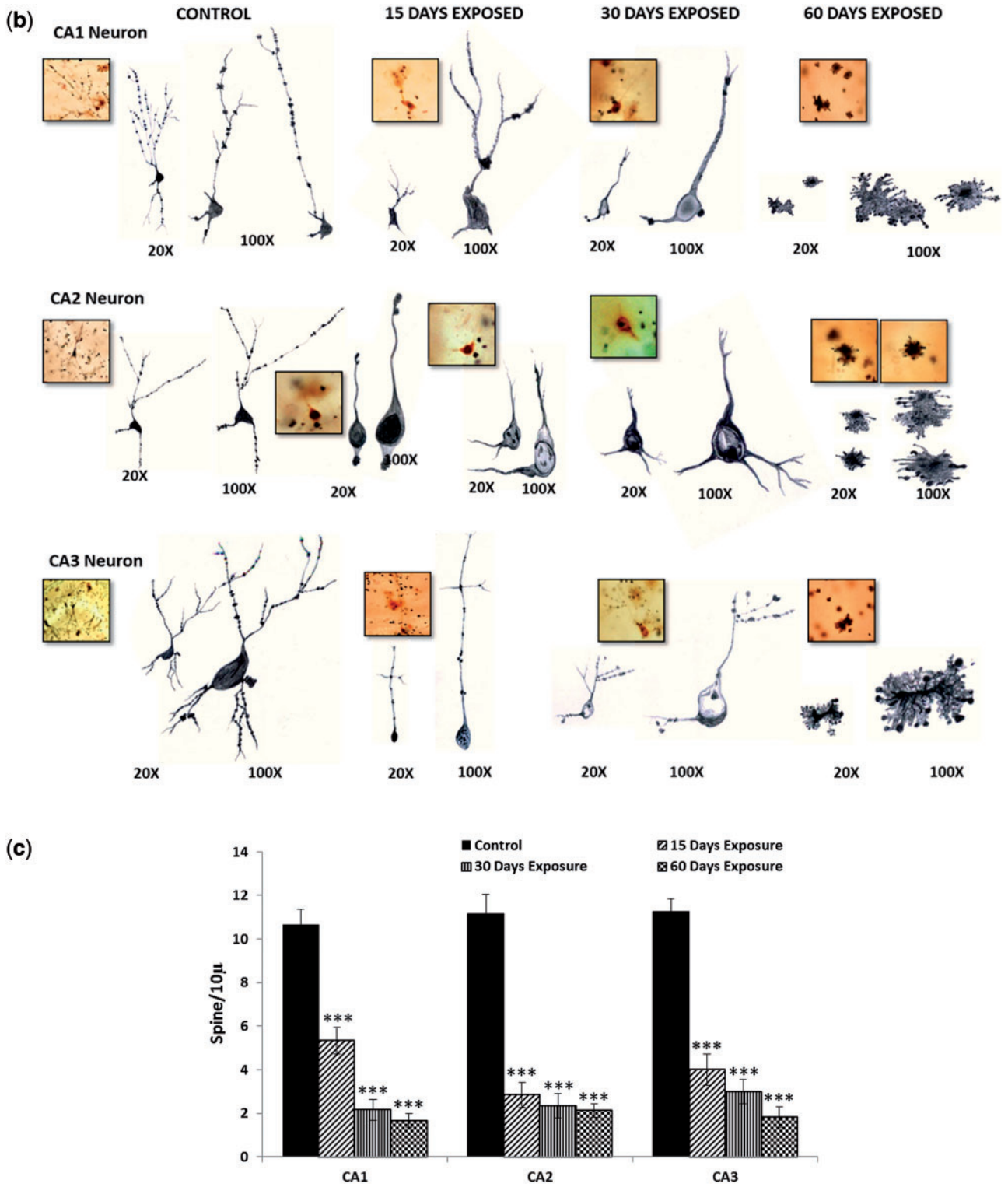

FIG. 3. Continued.

CW 2.45 GHz MW Irradiation for Different Time Duration Induce ROS Overproduction Leads to LPO and Carbonylation of Biological Macromolecules

The oxidative stress induced by the overproduction of free radicals result in LPO and carbonylation of biological macromolecules and hippocampus neuronal membrane due to high content of easily oxidizable PUFAs are vulnerable to oxidative damage, therefore next we have monitored the MDA level, the end product of LPO which increases during oxidative stress. Significant increased MDA level was observed in 15 ($P < .05$), 30 ($P < .01$), and 60 days ($P < .001$) 2.45 GHz MW radiation exposed group of mice compared with sham control (Figure 5A). Similar pattern for carbonyl content was observed in hippocampus (Figure 5B).

TABLE 1. Comparative Analysis of Number of Pyramidal Neurons, Average Soma Diameter and Axonal Length of Pyramidal as Well as Other Neurons in CA 1, CA 2, and CA 3 Regions of Hippocampus

Parameters	Hippocampal Area	Experimental Groups			
		Control	15 Days Exposed	30 Days Exposed	60 Days Exposed
No. of pyramidal Neurons/section	CA 1	11	5**	3***	—
	CA 2	12	3***	1***	—
	CA 3	5	3	1**	—
Soma Diameter (in μm)	CA 1	31.46 ± 3.63	48.13 ± 2.11*	56.68 ± 2.24**	66.37 ± 5.72**
	CA 2	48.55 ± 2.60	61.88 ± 1.64*	126.42 ± 5.83***	124.71 ± 5.97***
	CA 3	30.88 ± 1.54	47.87 ± 2.59**	53.65 ± 2.79**	59.09 ± 4.22**
Axonal length (in μm)	CA 1	779.16 ± 71.66	698.90 ± 63.79	336.69 ± 28.89**	86.93 ± 5.20***
	CA 2	522.11 ± 29.61	297.97 ± 27.04**	123.02 ± 14.27***	70.58 ± 6.51***
	CA 3	385.96 ± 27.96	322.32 ± 31.25	151.16 ± 15.57***	64.26 ± 3.54***

Each value represents the mean ± SEM ($N = 5$). Significance of the difference was determined by using 1-way ANOVA. *$P < .05$, **$P < .01$, and ***$P < .001$ significance of difference from control.

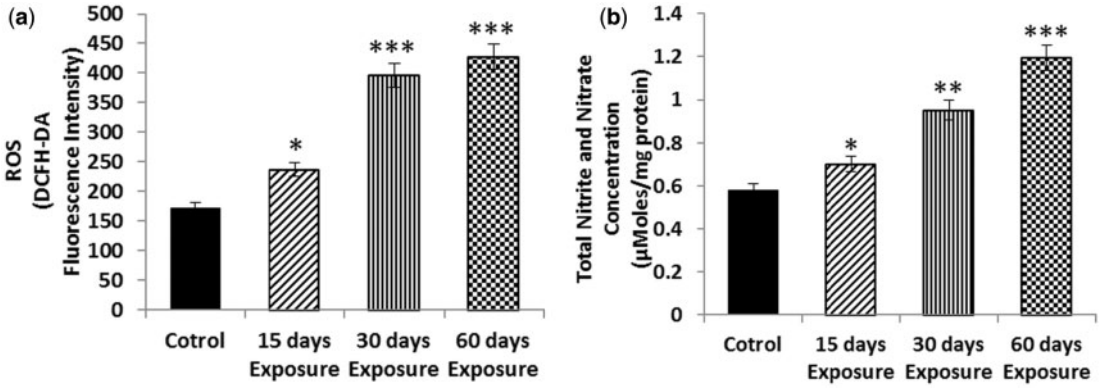

FIG. 4. Effect of 2.45 GHz MW radiation on (A) reactive oxygen species (ROS) measured by 2′7′-dichlorodihydrofluorescein diacetate (DCFH-DA) fluorescence intensity, and (B) total nitrite and nitrate concentration in hippocampus region of MW irradiated mice. Increased DCFH-DA intensity and total nitrite and nitrate concentration was observed in hippocampus of MW irradiated mice. Significant increase in both ROS and total nitrite and nitrate concentration was observed in all the 2.45 GHz (CW) MW radiation exposed group of mice than control. Results are expressed as mean ± SEM ($N = 10$). Significance of the difference was determined by using 1-way ANOVA. *$P < .05$, **$P < .01$, and ***$P < .001$ significance of difference from control.

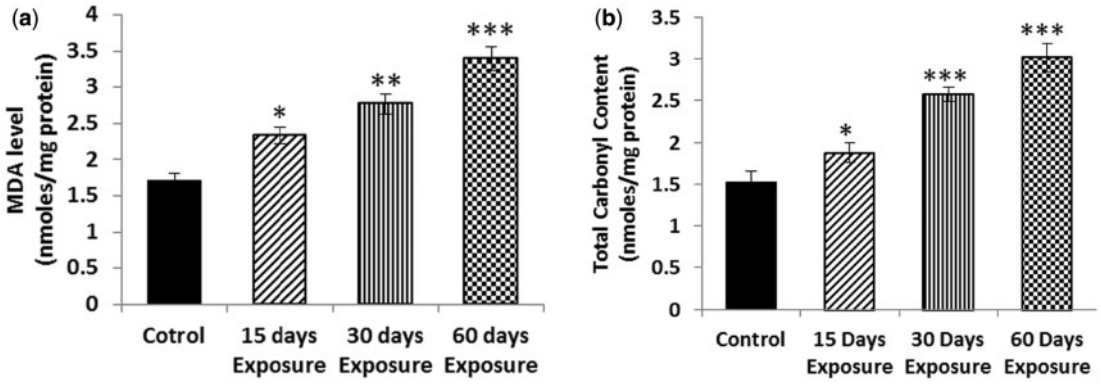

FIG. 5. Effect of 2.45 GHz (CW) MW radiation on (A) Level of peroxidized lipids (MDA: malondialdehyde); and (B) Total carbonyl content (oxidative damage to nucleic acids and proteins). Significant increase in MDA and total carbonyl content was observed in MW-exposed mice. Values are expressed as mean ± SEM ($N = 10$). Data were analyzed by data were analyzed by using 1-Way ANOVA. Significance of difference from control *$P < .05$, **$P < .01$, and ***$P < .001$.

CW 2.45 GHz MW Radiation for Different Time Duration Induce Increased ROS Production Results in Decreased ROS Scavenging Enzymes Activity

ROS-scavenging enzymes—SOD, CAT, and GPx—combinatorially play a major role in maintaining the intracellular concentration of ROS. These 3 antioxidant enzymes together with glutathione (GSH) form the first line of defense against ROS. Because elevated ROS production is responsible for reduced antioxidant enzyme activity, we further evaluate the antioxidant enzyme activity (SOD, CAT, and GPx) in hippocampus of different group animals. The activities of antioxidant enzymes were found to be decreased significantly in gradual

manner after short- and long-term 2.45 GHz MW irradiation and the degree of effect was more as the duration of exposure increased (Figure 6). The activity of SOD was found to be significantly decreased in the hippocampus of all the experimental groups, ie, 15 ($P < .05$), 30 ($P < .01$), and 60 days ($P < .001$) exposed group compared with sham control (Figure 6A). Significant decrease in CAT activity was also observed in 15 ($P < .01$), 30 ($P < .001$), and 60 days ($P < .001$) 2.45 GHz MW radiation exposed animals than sham control (Figure 6B). Similar trend of decrement was also observed in case of GPx activity after short- and long-term 2.45 GHz MW irradiation. Significant increase in GPx activity was observed in 15 days exposed mice ($P < .01$), 30 days ($P < .001$), and 60 days ($P < .001$) MW-irradiated animals than sham control (Figure 6C).

CW 2.45 GHz MW Radiation for Different Time Duration Decreased Creatine Kinase Activity in Hippocampus

CKs are important in maintaining cellular-energy homeostasis. It is involved in synthesis and metabolism of phosphocreatine (PCr), in the hippocampus, serves as an energy reservoir for the rapid buffering and regeneration of ATP. Studies suggest a role for the creatine- PCr/CK circuit in the formation or maintenance of hippocampal mossy fiber connections, and processes that involve spatial learning and memory. Therefore, next we measure the activity of CK in hippocampus. The activity of CK decreased after 15 days ($P < .05$), 30 days ($P < .001$), and 60 days ($P < .001$) exposure of 2.45 GHz MW radiation compared with sham control group (Figure 7).

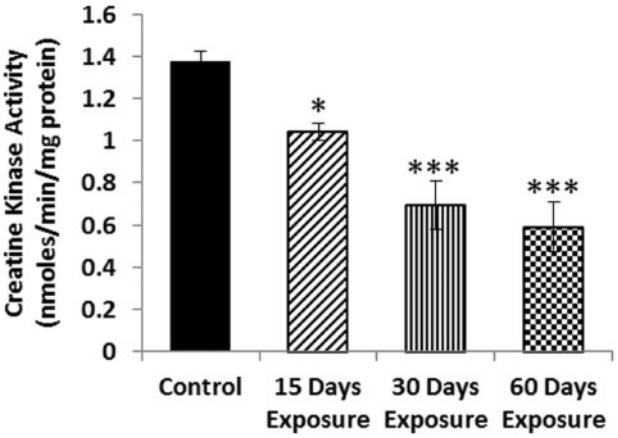

FIG. 7. Effect of 2.45 GHz (CW) MW irradiation on Creatine kinase activity in hippocampus. Significant decrease in Creatine kinase activity was observed in 15, 30, and 60 days MW exposed group. Values are expressed as mean ± SEM ($N = 10$). *$P < .05$, ***$P < .001$ significance of difference between group.

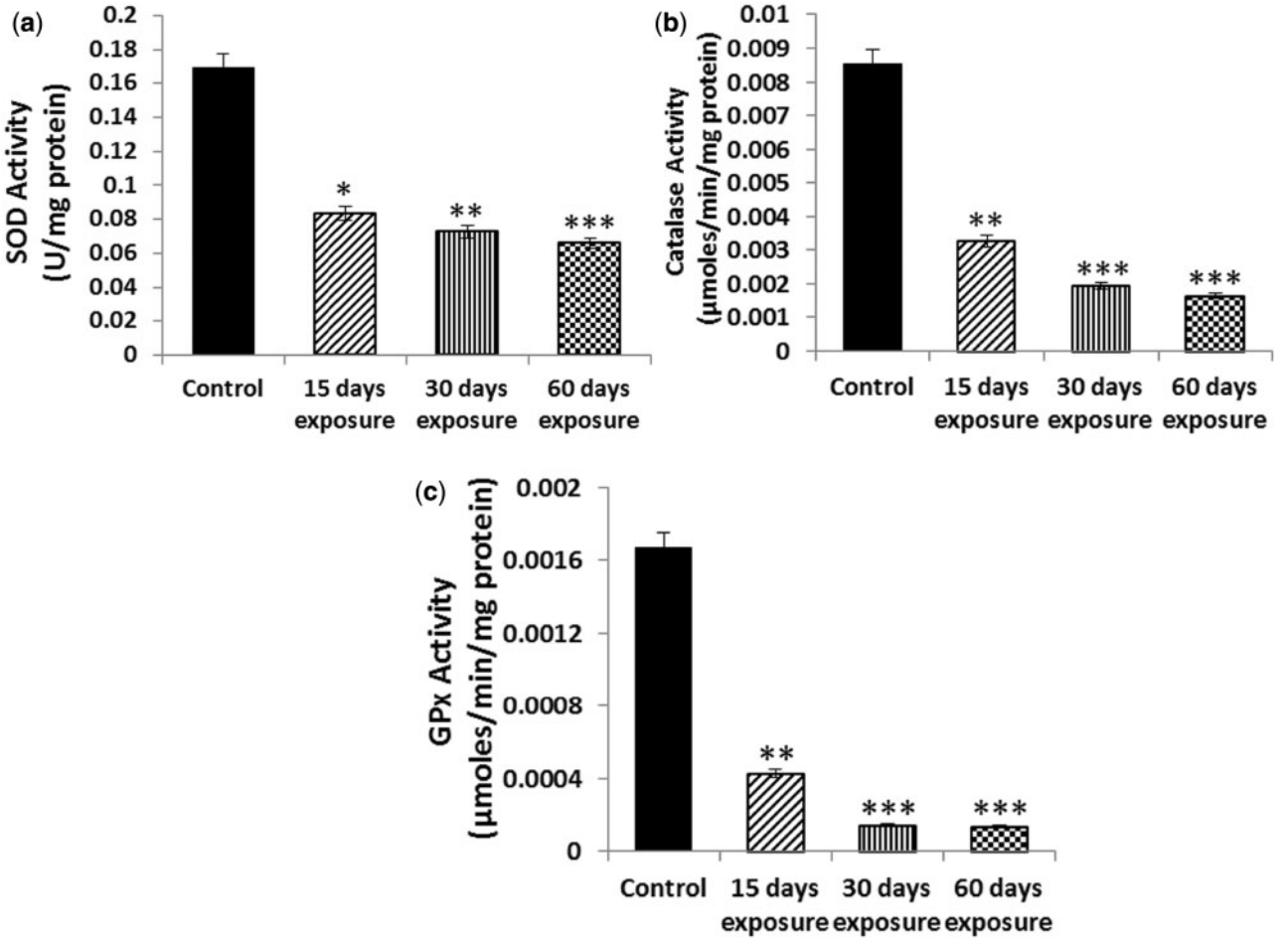

FIG. 6. Changes in Antioxidant enzymes activities (A) superoxide dismutase, (B) catalase, and (C) glutathione peroxidase of 2.45 GHz (CW) MW irradiated mice. 15, 30, and 60 days MW-exposed mice show significant decrease in all the antioxidant enzymes activity compared with control. Decreased antioxidant levels in MW irradiated group contribute to increased ROS generation in hippocampus and thus may lead to hippocampal neuronal and nonneuronal apoptosis. Values are expressed as mean ± SEM ($N = 10$). Significance of difference from control *$P < .05$, **$P < .01$, and ***$P < .001$.

Immunohistochemistry of Full Length p53, Bax, Pro-Caspase-3, and Full Length/Uncleaved PARP-1 in Hippocampal Neuronal and Nonneuronal Cell

To test the hypothesis whether 2.45 GHz (CW) MW irradiation induce neuron degeneration via p53-dependent/independent apoptosis, we have investigated p53 and Bax, a pro-apoptotic marker and inactive executioner Caspase-3 (pro-Caspase-3) and full length/uncleaved DNA repair enzyme PARP-1in hippocampal neurons (Figure 8). The expression of p53 (Figure 8A) and Bax (Figure 8B) in the neuronal and nonneuronal cell of DG, CA1, CA2, and CA3 of hippocampus was upregulated while the expression of pro-Caspase-3 (Figure 8C) and uncleaved PARP-1 (Figure 8D) were downregulated after 2.45 GHz MW irradiated in time-dependent manner. Control mice hippocampus showed weak immunoreactivity for p53 (Figure 8A, Table 2) and Bax (Figure 8B, Table 3), 15 days exposed mice revealed moderate immunostaining while 30 and 60 days exposed mice showed intense immunoreactivity for p53 and Bax, suggesting MW radiation induce p53-dependent/independent apoptosis of hippocampal neuronal and nonneuronal cells. Intense immunostaining for pro-Caspase-3 (Figure 8C, Table 4) and uncleaved PARP-1 (Figure 8D, Table 5) was observed in sham control while the experimental group revealed moderate and weak staining for pro-Caspase-3 and uncleaved PARP-1 in the neuronal and nonneuronal cell of different region of hippocampus.

DISCUSSION

The applications of MW emitting devices are increasing day by day in our daily life. MW oven, mobile phone, Wi-Fi, etc. have become the integral necessary part of our life and thus raised a strong health concerned issues. Studies suggest that MW radiation affects the brain physiology and function (Joubert *et al.*, 2008; McRee and Wachtel, 1980; Salford *et al.*, 2003) and could cause the spatial memory impairment (Lai *et al.*, 1994; Wang and Lai, 2000). However, the underlying mechanisms through which MW radiation exerts its neurotoxic effect responsible for cognitive dysfunction have not been well understood yet. This study documents the temporal impact of low level 2.45 GHz (CW) MW radiation (overall average Power density = 0.0248 mW/cm^2 and overall average whole body SAR value = 0.0146 W/Kg) on the hippocampus with special reference to spatial learning and memory. Hippocampus is responsible for the integration of spatial learning and memory information (Vorhees and Williams 2006). It is responsible for encoding, storage, consolidation, and retrieval of spatial memory. It is formed of subfields of DG, CA3, CA2, and CA1 to receive highly processed information from widespread neocortical regions through 3 temporal cortical areas known as the entorhinal, perirhinal, and postrhinal cortices, and through other direct projections from extratemporal areas (Bird and Burgess, 2008). The main relay station for the transmission of sensory information to the hippocampus is the entorhinal cortex which provides a substantial input to the DG, which, in turn, provides the major input to CA3 via the mossy fiber projection. CA3 provides the major input to CA1 via CA2 (Bannerman *et al.*, 2014; Bird and Burgess, 2008; Neves *et al.*, 2008).

Our results demonstrate that MW radiation exposure resulted in spatial memory impairment due to hippocampal neuronal and nonneuronal cells degeneration which increases with the duration of MW radiation exposure. Thirty and 60 days of 2.45 GHz (CW) MW radiation exposure exhibited pronounced spatial memory impairment in Morris water maze task.

In addition to memory deficit, the MW exposure reduced number of pyramidal neurons, neuronal soma diameter, axonal length, neuronal arborization, and number of dendritic spines in a time-dependent manner may be due to increase in cellular oxidative/nitrosative stress (ROS and NO levels, LPO, and PCOs) along with a decreased ROS scavenging antioxidant enzymes (SOD, CAT, and GPx) activity in the hippocampus. Reduced antioxidant enzymes activity in the hippocampus is directly related to the elevated level of ROS/RNS, MDA (index of LPO), and TCO contents (index of DNA/protein oxidation) which may lead to prolonged neuronal dysfunction (Ates *et al.*, 2006). Because, hippocampal CA1, CA 2, and CA 3 neurons are known to play a major role in spatial memory (Suh *et al.*, 2011) therefore, the decrease in apical spine number in MW irradiated mice may decline spatial memory. In this study, as MW irradiated mice showed significant deficit in the MWM task, which indicates learning and spatial memory impairment may be due to the structural and functional loss of integrity of the hippocampus (Burke and Barnes, 2010; Lalonde, 2002). The reduced neuronal arborization, spine number, and subsequent neurodegeneration may lead to inadequate long-term potentiation resulting in the impairment of learning and spatial memory (Sanders *et al.*, 2000).

This study demonstrates consistently overproduction of free radicals led to increased carbonyl contents and LPO derivatives in hippocampus. MW radiation exposure of 2 h/day for 15, 30, and 60 days showed time-dependent increment in free radical load which subsequently induce the oxidative and nitrosative stress, and weaken the antioxidant defense system in hippocampus. The free radical load may also lead to the severe oxidative damage to cellular constituent's viz. LPO derivatives and carbonyls. Report from our laboratory suggest that MW radiation cause DNA single strand break/double strand break (DSB) in the brain (Chaturvedi *et al.*, 2011; Shahin *et al.*, 2013). In apoptotic neurodegenerative processes, oxidative stress plays a key role, along with metabolic compromise and excitotoxicity (Alexi *et al.*, 2000). It has been documented that brain cells are more vulnerable to ROS and RNS-mediated oxidative damage because of the following facts, ie, high rate of oxygen consumptions, high content of metals such as iron, catalyzing free radical formation, and low concentrations of antioxidants to combat oxidative stress (Ikonomidou and Kaindl, 2011). Moreover, neuronal membrane has high content of easily oxidizable PUFAs. MW irradiation generated free radicals may react with the neuronal PUFAs resulting in peroxidation which finally leads to structural and functional disruption of the neuronal cell membrane. Increasing evidences have also shown that, structural and functional disruption of the cell membrane and enzyme inactivation is the outcome of oxidative damage to lipids (LPO) and proteins (protein oxidation) (Avrova *et al.*, 1998). These findings, in brief, suggest that the memory impairment in MW irradiated mice might be due to MW radiation induced oxidative damage to hippocampal neuronal and nonneuronal cells.

Another important observation of our study was significant decrease in hippocampal CK activity along with the MW exposure duration suggesting a potential energy deficiency in neurons. Because PCr-CK system is known to play a vital role in neuronal energy homeostasis, optimal CK activity is critical for proper neuronal functioning (Wallimann *et al.*, 2011). It plays a crucial role in the production and maintenance of energy in neuronal cells. Brain-CK is a target of ROS (Choi *et al.*, 2001). Oxidative modification of CK inhibits its activity due to proteasome-mediated degradation (Hara *et al.*, 2012). The alterations

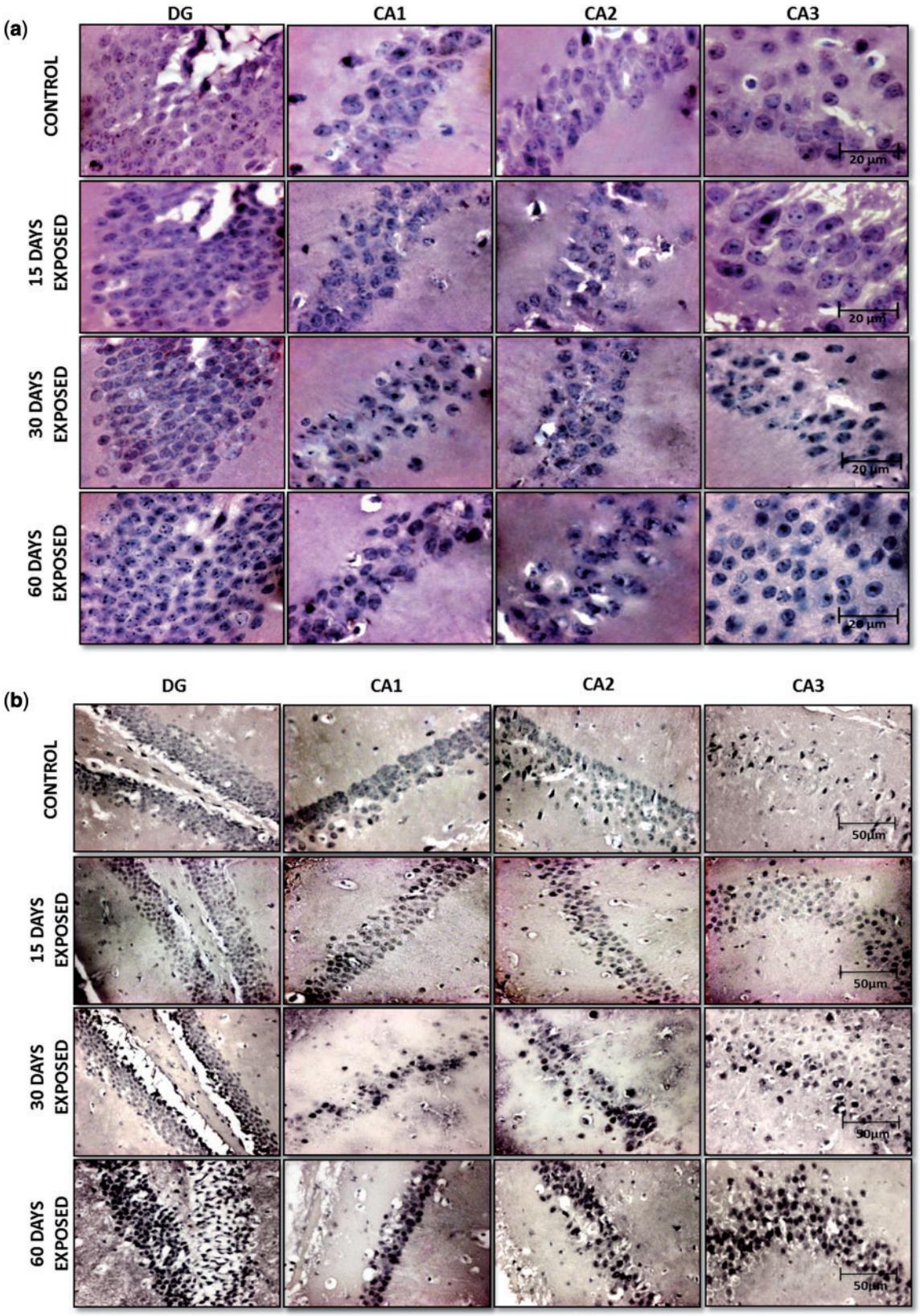

FIG. 8. Immunohistochemistry of (A) full length p53, (B) Bax, (C) pro-Caspase-3, and (D) full length/uncleaved Poly (ADP-ribose) polymerase (PARP-1) in mice hippocampal neuron of CA1, CA2, CA3, and DG. The expression of p53 and Bax were found to be upregulated and pro-caspase-3 and uncleaved PARP-1 was downregulated in all the regions of hippocampus of 2.45 GHz (CW) MW irradiated mice temporally with the exposure duration in time-dependent manner. The alterations in these pro-apoptotic proteins, executioner caspase (pro-Caspase 3), and DNA repair enzyme (full length PARP-1) may lead to hippocampal neurodegeneration.

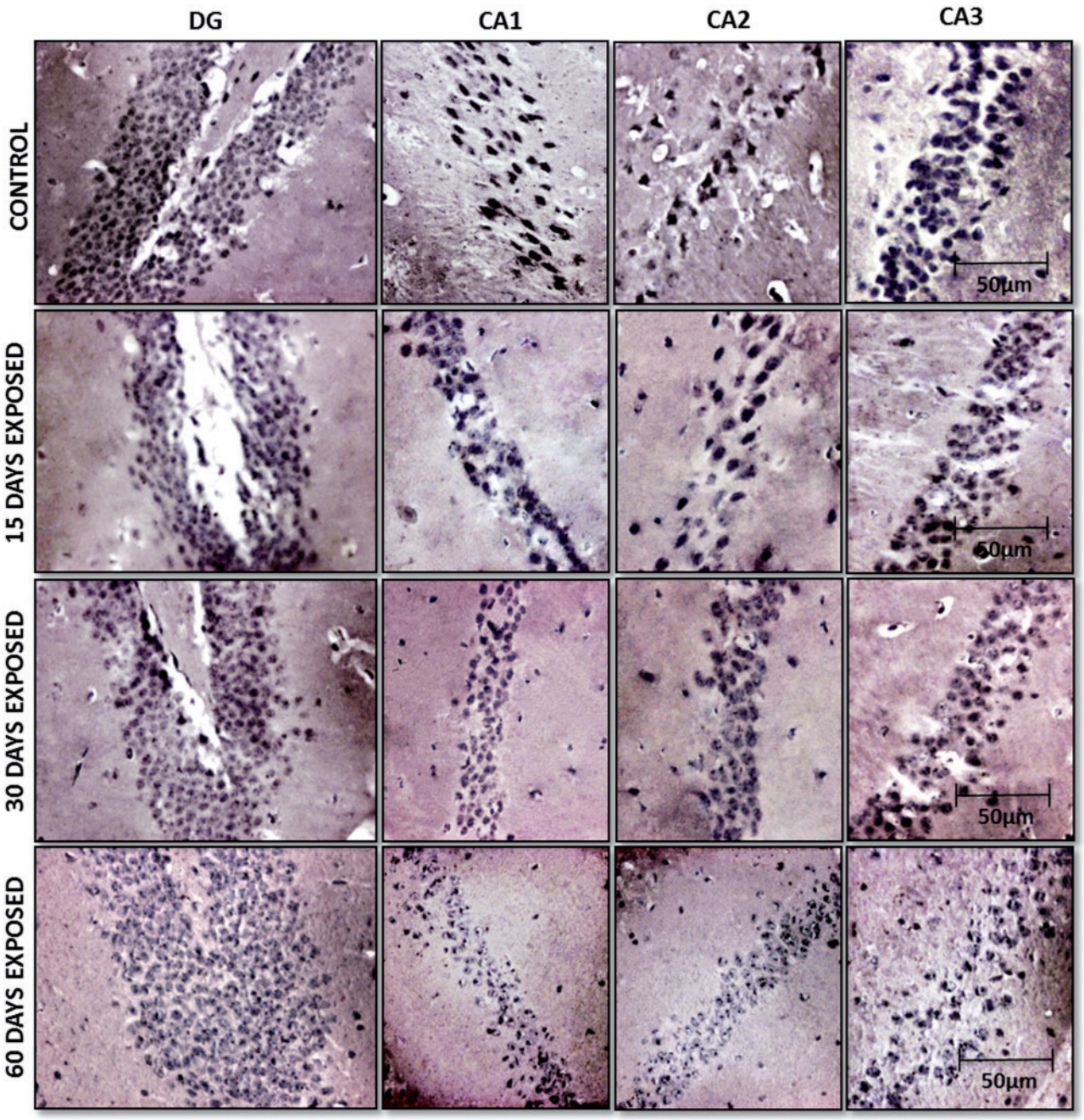

FIG. 8. Continued.

of mitochondrial permeability with consequent reduction of ATP supply enable cells to undergo apoptosis or other form of programmed cell death (Guimaraes and Linden, 2004).

Therefore, MW radiation induced oxidative and nitrosative stress inhibits the hippocampal CK activity and as a consequence the cellular energy status of glia cells, neurons, and synaptic elements is perturbed. Altogether, we suggest that the MW irradiation induced impaired redox status and energy imbalance in the hippocampus will eventually lead to neuronal and nonneuronal cell death which will eventually contribute to cognitive dysfunction and memory impairment.

Our study also demonstrates an increase in the expression of both p53 and Bax protein along with a decrease in pro-Caspase-3 and uncleaved PARP-1 expression in hippocampal neuronal and nonneuronal cells of MW irradiated mice with increased exposure time duration. p53 is a pivotal molecule regulating the death of neurons. It get stabilized and activated in response to DNA damage by at least 2 partially independent pathways, one of which responds to DNA DSBs. Second one is activated by bulky lesions in DNA (Agarwal *et al.*, 1998). p53-mediated apoptosis can occur either by upregulating Bax activity or downregulating Bcl-2 activity. p53 becomes active after facing with DNA damage and stimulates the Bax, which warps the Bcl-2:Bax ratio. However, duality in p53 alternates between trans-activation and trans-repression. If the Bax level is constitutively high, p53 may mediate apoptosis through a

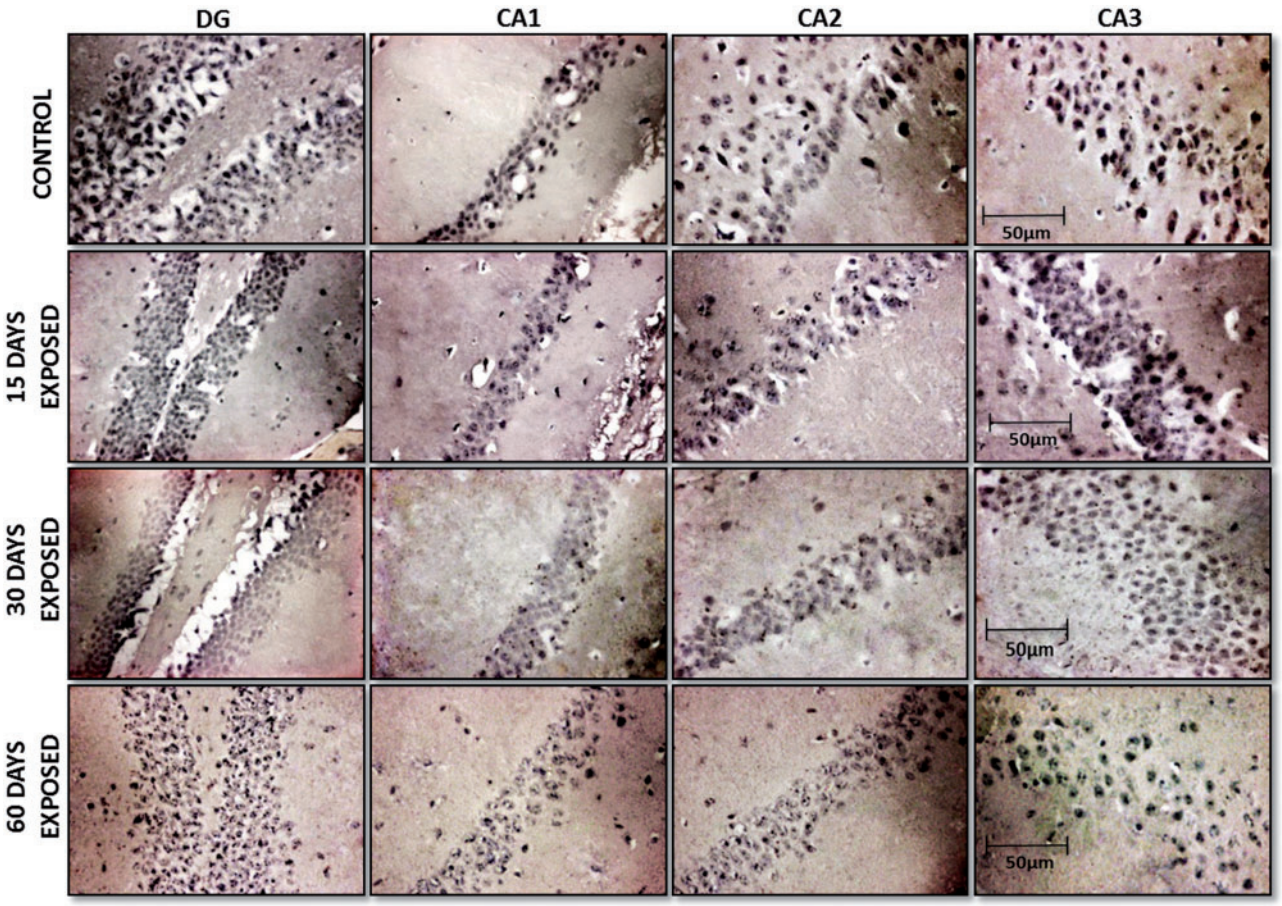

FIG. 8. Continued.

transcriptionally independent pathway. Bax also promotes apoptosis by binding to and antagonizing the Bcl-2 protein. We suggest that overexpression of p53 accompanies Bax expression and similar findings have been shown to induce apoptosis in many cell types. This implies that p53-dependent/independent neuronal apoptosis is Bax dependent/mediated. On the basis of Bax upregulation and pro-Caspase-3 downregulation, we suggest that the decreased ratio of Bcl-2/Bax activate the executioner Caspase-3, via the cleaving of pro-Caspase-3 to Caspase-3. The effector caspase, active Caspase-3 may cleave its substrate after receiving signal from the initiator caspases. The target proteins include the nuclear protein/DNA repair enzyme, PARP-1. In addition to inducing protein degradation, activated Caspase-3 can degrade DNA via proteolytic activation of DNases (Liu *et al.*, 1998). These varieties of degradation trigger the execution of apoptosis. Therefore, the decreased expression of pro-Caspase-3 in all 2.45 GHz (CW) MW exposed group, suggest the cleavage of inactive Caspase-3/pro-Caspase-3 into active Caspase-3. The active Caspase-3 cleaved full length/uncleaved PARP-1 in the nucleus, stalls the DNA repair and cell-cycle progression and thus mediate the hippocampal neuronal and non-neuronal apoptosis. Another, possibility is that the cellular stress results in the elevation of the Bax which permeabilizes the mitochondrial outer membrane and releases the apoptotic proteins (eg, cytochrome c) for diffusion in cytosol and subsequently serves in the activation of executioner Caspase-3 which ultimately leads to apoptosis. The ability of MW irradiation to induce p53 and to produce apoptosis in hippocampal neurons, as demonstrated in our studies, is also consistent with a role for these proteins in hippocampal neuronal apoptosis.

Altogether, we can suggest that MW irradiation results in the oxidative and nitrosative stress induced overexpression of p53 which stimulate the expression of Bax, downregulation of pro-Caspase-3, and full length/uncleaved PARP-1 which eventually leads to neuron degeneration via apoptosis. This will results in cognitive dysfunction and memory impairment. Our study shows that the temporal development of anatomical and behavioral abnormalities following the chronic low level 2.45 GHz (CW) MW irradiation exposure produce cell dysfunction and cell death in hippocampus. This exposure for prolong duration may result in neurodegeneration, ie, loss of structure and function of hippocampal neurons. In our study low level 2.45 GHz (CW) MW exposure for 15, 30, and 60 days describe progressive neuronal loss and ultimately impairs the learning and spatial memory. The neurological consequence of neurodegeneration following the 2.45 GHz MW radiation exposure may have devastating effects on mental and physical functioning.

Further, the observed effects of 2.45 GHz (CW) MW irradiation may be due to the possible microthermal effects which are inconsonance with the observations of De Pomerai and his group (Dawe *et al.*, 2006). The mouse brain which is composed of multiple structural layers, there may be reflection of low-level MWs at the interfaces of these layers resulting in hot spot formation which can induce observed microthermal effects in mouse hippocampus and can thus lead to neurodegeneration through p53-dependent/independent Bax-mediated apoptosis.

TABLE 2. Full Length p53 Immunoreactivity in Neuronal and Nonneuronal Cells of Different Hippocampal Area (DG, CA1, CA2, and CA3)

Hippocampal Area	DG				CA 1				CA 2				CA 3			
Experimental Groups	Cont.	15 days Exposed	30 days Exposed	60 days Exposed	Cont.	15 days Exposed	30 days Exposed	60 days Exposed	Cont.	15 days Exposed	30 days Exposed	60 days Exposed	Cont.	15 days Exposed	30 days Exposed	60 days Exposed
Total *ir*-cells	22.5 ± 2.78	60 ± 3.24***	85.75 ± 2.92***	121.25 ± 5.32***	17 ± 1.95	32.75 ± 1.75**	46 ± 2.48***	55.5 ± 2.39***	14 ± 1.58	29.75 ± 0.85**	32.25 ± 2.01**	42.5 ± 4.17**	10.5 ± 1.55	30.5 ± 2.32*	47.5 ± 3.79**	68.5 ± 3.12***
Intense *ir*-cells	6 ± 2.60	13 ± 1.92	26 ± 3.13**	58 ± 4.68***	5 ± 2.17	9 ± 2.90	20 ± 2.37**	30 ± 1.92***	4 ± 1.10	4 ± 0.32	15 ± 1.72**	30 ± 3.21**	1 ± 0.002	7 ± 1.42	31 ± 2.11**	35 ± 2.14***
Moderate *ir*-cells	8 ± 3.47	15 ± 2.21	32 ± 3.85**	46 ± 3.71***	2 ± 0.34	17 ± 1.36*	18 ± 3.91*	16 ± 2.16**	5 ± 1.72	12 ± 1.46**	10 ± 1.04	10 ± 0.41*	2 ± 0.02	18 ± 1.27*	8 ± 1.86	32 ± 1.56***
Weak *ir*-cells	9 ± 3.91	40 ± 5.88***	25 ± 2.01**	20 ± 1.61*	10 ± 1.23	6 ± 1.63	8 ± 1.09	9 ± 1.01	5 ± 1.51	13 ± 0.53	8 ± 0.084	2 ± 0.03	3 ± 0.019	4 ± 1.37	4 ± 0.098	7 ± 0.014

Each value represents the mean ± SEM ($N = 5$). Significance of the difference was determined by using 1-way ANOVA. *$P < .05$, **$P < .01$, and ***$P < .001$ significance of difference from control.

TABLE 3. Bax Immunoreactivity in Neuronal and Nonneuronal Cells of Different Hippocampal Area (DG, CA1, CA2, and CA3)

Hippocampal Area	DG				CA 1				CA 2				CA 3			
Experimental Groups	Cont.	15 days Exposed	30 days Exposed	60 days Exposed	Cont.	15 days Exposed	30 days Exposed	60 days Exposed	Cont.	15 days Exposed	30 days Exposed	60 days Exposed	Cont.	15 days Exposed	30 days Exposed	60 days Exposed
Total *ir*-cells	63.5 ± 4.33	154.25 ± 13.54**	262.75 ± 4.48***	279.25 ± 7.36***	23.75 ± 3.94	49 ± 3.13***	61.75 ± 3.68***	93 ± 3.53***	28 ± 3.14	60.25 ± 2.59**	64.75 ± 2.56***	88 ± 2.86***	39 ± 2.68	72.75 ± 5.91***	94.5 ± 5.63***	131 ± 3.85***
Intense *ir*-cells	24 ± 3.87	65 ± 3.36*	136 ± 6.14***	225 ± 15.32***	4 ± 0.57	25 ± 2.52***	37 ± 3.25***	43 ± 2.67***	8 ± 3.02	10 ± 2.17	35 ± 2.13***	63 ± 4.31***	27 ± 1.63	30 ± 3.75	48 ± 3.01**	101 ± 4.62***
Moderate *ir*-cells	13 ± 1.12	119 ± 6.16***	98 ± 4.97**	30 ± 2.78**	5 ± 0.031	12 ± 1.13*	10 ± 0.76	35 ± 2.85**	10 ± 1.58	40 ± 3.25**	15 ± 1.94	20 ± 1.89	5 ± 0.12	40 ± 2.97***	30 ± 2.11***	26 ± 2.13*
Weak *ir*-cells	25 ± 1.41	9 ± 0.65	29 ± 2.16	17 ± 1.72	14 ± 1.02	10 ± 1.06	14 ± 0.057	15 ± 2.13	10 ± 2.98	10 ± 1.97	14 ± 1.18	5 ± 0.043	12 ± 1.52	22 ± 2.11	16 ± 0.56	4 ± 0.045

Each value represents the mean ± SEM ($N = 5$). Significance of the difference was determined by using 1-way ANOVA. *$P < .05$, **$P < .01$, and ***$P < .001$ significance of difference from control.

TABLE 4. Pro-Caspase-3 Immunoreactivity in Neuronal and Nonneuronal Cells of Different Hippocampal Area (DG, CA1, CA2, and CA3)

Hippocampal Area	DG				CA 1				CA 2				CA 3			
Experimental Groups	Cont.	15 days Exposed	30 days Exposed	60 days Exposed	Cont.	15 days Exposed	30 days Exposed	60 days Exposed	Cont.	15 days Exposed	30 days Exposed	60 days Exposed	Cont.	15 days Exposed	30 days Exposed	60 days Exposed
Total *ir*-cells	173 ± 4.67	147.5 ± 3.23*	102.75 ± 5.17***	90.5 ± 3.62***	71.5 ± 3.62	55.75 ± 2.09*	45.25 ± 2.59***	47.25 ± 3.14***	56.5 ± 2.78	35.5 ± 2.22*	30.5 ± 1.94**	28.25 ± 3.09**	94 ± 2.64	80 ± 2.27**	54.5 ± 3.12***	45.5 ± 3.62***
Intense *ir*-cells	70 ± 3.91	35 ± 2.98*	20 ± 2.27***	8 ± 0.097***	55 ± 3.18	39 ± 2.61*	12 ± 1.15***	10 ± 1.19***	25 ± 2.47	20 ± 1.83	5 ± 0.18***	5 ± 0.23***	72 ± 3.49	39 ± 2.91**	20 ± 2.12***	5 ± 1.95***
Moderate *ir*-cells	62 ± 2.15	50 ± 2.79	39 ± 2.92*	22 ± 2.21*	12 ± 2.36	12 ± 1.45	11 ± 1.37	15 ± 2.11	21 ± 1.98	7 ± 0.32*	17 ± 2.14	8 ± 0.12**	16 ± 2.09	32 ± 2.97*	27 ± 3.33	8 ± 0.13
Weak *ir*-cells	40 ± 1.17	62 ± 0.072	42 ± 1.32	60 ± 1.73	4 ± 0.097	8 ± 0.21	22 ± 2.55**	22 ± 1.32**	10 ± 1.86	8 ± 0.27	8 ± 0.12	10 ± 0.12	5 ± 0.32	9 ± 1.53	7 ± 0.28	32 ± 0.92***

Each value represents the mean ± SEM ($N = 5$). Significance of the difference was determined by using 1-way ANOVA. *$P < .05$, **$P < .01$, and ***$P < .001$ significance of difference from control.

TABLE 5. Full Length/Uncleaved PARP-1 Immunoreactivity in Neuronal and Nonneuronal Cells of Different Hippocampal Area (DG, CA1, CA2, and CA3)

Hippocampal Area	DG				CA 1				CA 2				CA 3			
Experimental Groups	Cont.	15 days Exposed	30 days Exposed	60 days Exposed	Cont.	15 days Exposed	30 days Exposed	60 days Exposed	Cont.	15 days Exposed	30 days Exposed	60 days Exposed	Cont.	15 days Exposed	30 days Exposed	60 days Exposed
Total *ir*-cells	114.5 ± 9.18	69.5 ± 2.10**	54.75 ± 3.75***	50 ± 2.48***	60 ± 3.29	28.25 ± 2.93***	16 ± 1.68***	14 ± 0.91***	57 ± 3.94	44.75 ± 2.56*	22.5 ± 2.10***	25 ± 1.08***	95 ± 2.55	71.5 ± 3.79**	50 ± 3.81***	46 ± 2.79***
Intense *ir*-cells	72 ± 3.51	22 ± 2.28**	16 ± 2.92***	10 ± 1.37***	32 ± 2.91	8 ± 1.36**	5 ± 0.032***	3 ± 0.84***	25 ± 3.73	10 ± 1.43*	3 ± 0.17***	4 ± 1.34***	60 ± 3.89	30 ± 3.25	8 ± 0.61***	5 ± 2.13***-
Moderate *ir*-cells	26 ± 2.99	25 ± 3.66	14 ± 3.15	15 ± 2.26*	18 ± 1.32	7 ± 2.11	4 ± 1.83*	4 ± 0.87*	12 ± 2.12	19 ± 1.22	2 ± 0.032*	7 ± 0.78	25 ± 3.31	24 ± 2.92	20 ± 2.27	26 ± 2.65
Weak *ir*-cells	16 ± 1.77	13 ± 1.24	24 ± 1.26*	25 ± 3.21*	14 ± 1.62	13 ± 2.16	10 ± 1.49	17 ± 1.15	20 ± 2.50	15 ± 0.56	17 ± 1.28	14 ± 1.84	10 ± 0.29	17 ± 0.98	40 ± 4.52***	15 ± 0.03

Each value represents the mean ± SEM ($N = 5$). Significance of the difference was determined by using 1-way ANOVA. *$P < .05$, **$P < .01$, and ***$P < .001$ significance of difference from control.

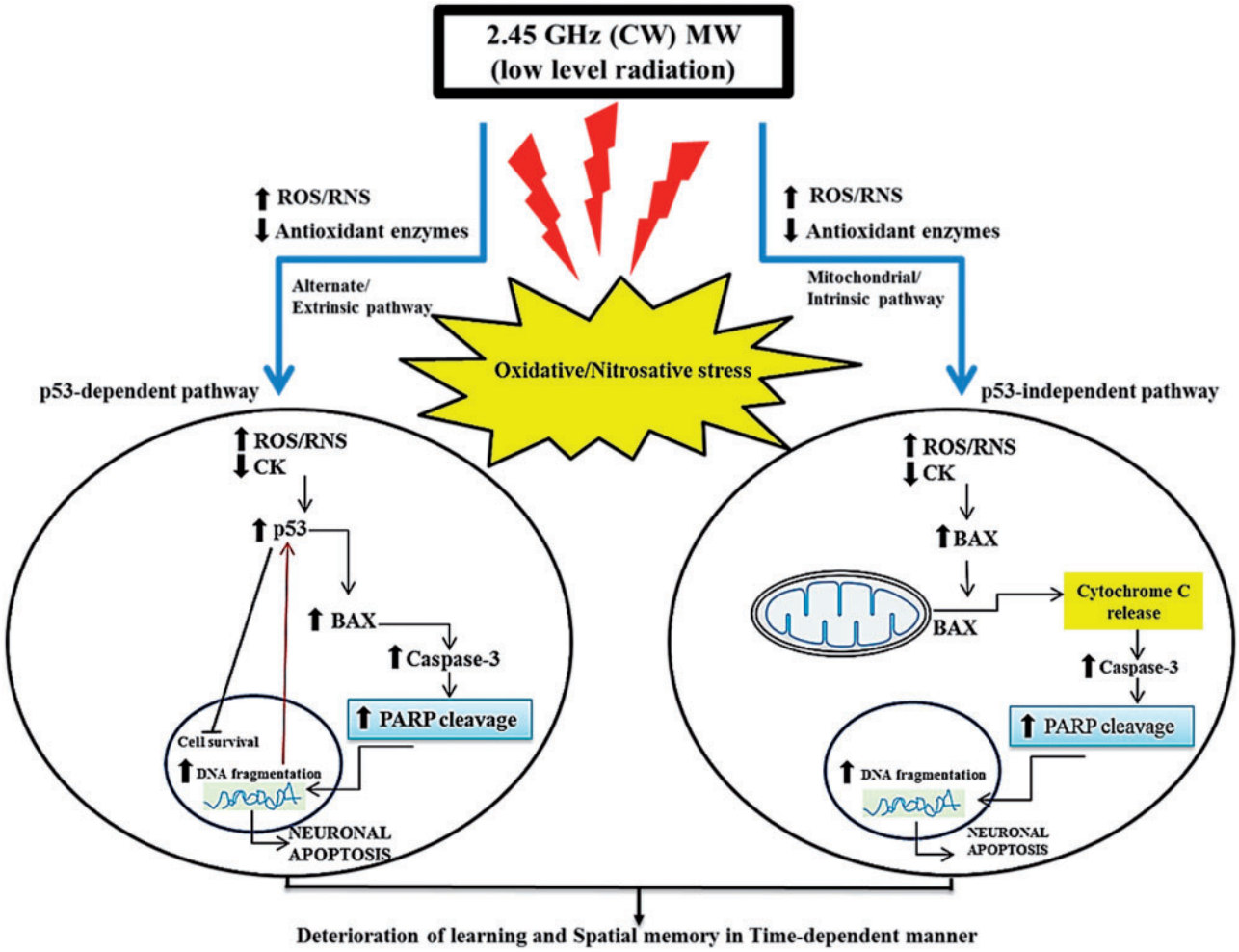

FIG. 9. Schematic depicting the 2.45 GHz (CW) MW radiation induced hippocampal neuronal and nonneuronal apoptosis mediated via oxidative/nitrosative stress induced p53-dependent/independent pathway. This model includes the findings on the pathways leading the hippocampal neuronal and nonneuronal apoptosis as observed in this study.

The role of low level 2.45 GHz (CW) MW irradiation in neurodegeneration has long been suspected. Although, the first step in recognizing the effect of short-and long-term 2.45 GHz (CW) MW radiation exposure results in correlating the deterioration in learning and spatial memory with exposure time duration. Such understanding is required to best estimate the risk of exposure. Findings and implementing novel treatments that are curative or at least reduce the neurodegeneration progression following the low level 2.45 GHz (CW) MW irradiation would be one of the most pressing research needs.

CONCLUSION

Our findings, in brief, conclude that the MW radiation induced oxidative and nitrosative stress results in the hippocampal neuronal and nonneuronal apoptosis via the oxidative damage of cellular constituents (viz. nucleic acids, proteins, and lipids) and subsequent overexpression of p53 which upregulate Bax as well as downregulate pro-Caspase-3 and full length/uncleaved PARP-1 which eventually lead to neuronal degeneration via apoptosis. As the duration of the chronic exposure (2 h/day) increases, 2.45 GHz (CW) MW irradiation mediates neuronal and nonneuronal cell death/apoptosis more severely in DG, CA1, CA2, and CA3. MW exposure also results in the reduction in the number of pyramidal neurons, neuronal soma and axonal length, neuronal arborization and dendritic spine number in the aforementioned areas of hippocampus. Neuronal and nonneuronal cell death along with the reduction in neuronal arborization and dendritic spines may lead to inadequate long-term potentiation and thus lead to the impairment in learning and spatial memory. These findings led us to conclude that chronic exposure to low level 2.45 GHz (CW) MW radiation severely affects the hippocampal neuronal plasticity and circuitry, and impairs learning and spatial memory through p53-dependent/independent apoptosis of hippocampal neuronal and nonneuronal cells (Figure 9).

Finally, further research is needed in identifying the potential biomarkers and new therapeutics in a model, at a stage where therapeutic target would be neurodegeneration modifying. To do so, the knowledge of the relevant doses of this low level 2.45 GHz (CW) MW radiation in our environment and the assessment of the role of this environmental toxicant in hippocampal neurodegeneration can accomplish in a way that is meaningful to human health and radiation exposures.

ACKNOWLEDGEMENT

This work was funded by a research grant (5/10/FR/13/2010-RHN) from the Indian Council of Medical Research (ICMR),

New Delhi, India to CMC and ICMR Senior Research Fellowship (45/2/2012-PHY/BMS) to Saba Shahin. We are grateful to Prof. Sukala Prasad, Biochemistry Unit, Department of Zoology, Banaras Hindu University, Varanasi, India for providing Morris Water Maze set-up facility.

REFERENCES

Aebi, H. (1984). Catalase in vitro. *Methods Enzymol.* **105**, 121.

Agarwal, M. L., Taylor, W. R., Chernov, M. V., Chernova, O. B., and Stark, G. R. (1998). The p53 network. *J. Biol. Chem.* **273**, 1–4.

Aksenov, M., Aksenova, M., Butterfield, D. A., and Markesbery, W. R. (2000). Oxidative modification of creatine kinase BB in Alzheimer's disease brain. *J. Neurochem.* **74**, 2520–2527.

Alexi, T., Borlongan, C. V., Faull, R. L., Williams, C. E., Clark, R. G., Gluckman, P. D., and Hughes, P. E. (2000). Neuroprotective strategies for basal ganglia degeneration: Parkinson's and Huntington's diseases. *Prog. Neurobiol.* **60**, 409–470.

Ansari, M. A., Joshi, G., Huang, Q., Opii, W. O., Abdul, H. M., Sultana, R., and Butterfield, D. A. (2006). In vivo administration of D609 leads to protection of subsequently isolated gerbil brain mitochondria subjected to in vitro oxidative stress induced by amyloid beta-peptide and other oxidative stressors: Relevance to Alzheimer's disease and other oxidative stress-related neurodegenerative disorders. *Free Radic. Biol. Med.* **41**, 1694–1703.

Ates, O., Cayli, S., Gurses, I., Yucel, N., Iraz, M., Altinoz, E., Kocak, A., and Yologlu, S. (2006). Effect of pinealectomy and melatonin replacement on morphological and biochemical recovery after traumatic brain injury. *Int. J. Dev. Neurosci.* **24**, 357–363.

Avrova, N. F., Victorov, I. V., Tyurin, V. A., Zakharova, I. O., Sokolova, T. V., Andreeva, N. A., Stelmaschuk, E. V., Tyurina, Y. Y., and Gonchar, V. S. (1998). Inhibition of glutamate-induced intensification of free radical reactions by gangliosides: Possible role in their protective effect in rat cerebellar granule cells and brain synaptosomes. *Neurochem. Res.* **23**, 945–952.

Bannerman, D. M., Sprengel, R., Sanderson, D. J., McHugh, S. B., Rawlins, J. N. P., Monyer, H., and Seeburg, P. H. (2014). Hippocampal synaptic plasticity, spatial memory and anxiety. *Nat. Rev. Neurosci.* **15**, 181–192.

Bejma, J., Ramires, P., and Ji, L. L. (2000). Free radical generation and oxidative stress with ageing and exercise: Differential effects in the myocardium and liver. *Acta Physiol. Scand.* **169**, 343–351.

Bird, C. M., and Burgess, N. (2008). The hippocampus and memory: Insights from spatial processing. *Nat. Rev. Neurosci.* **9**, 182–194.

Bivik, C. A., Larsson, N., Kagedal, K. M., Rosdahl, I. K., and Ollinger, K. M. (2006). UVA/B37 Induced Apoptosis in Human Melanocytes Involves Translocation of Cathepsins and 38 Bcl-2 Family Members. *J Invest Dermatol.* **126**, 1119–1127.

Bressler, J. P., Olivi, L., Cheong, J. H., Kim, Y., Maerten, A., and Bannon, D. (2007). Metal transporters in intestine and brain: Their involvement in metal-associated neurotoxicities. *Hum. Exp. Toxicol.* **26**, 221–229.

Burke, S. N., and Barnes, C. A. (2010). Senescent synapses and hippocampal circuit dynamics. *Trends Neurosci.* **33**, 153–161.

Butterfield, D. A., Castegna, A., Lauderback, C. M., and Drake, J. (2002). Evidence that amyloid β-peptide induced lipid peroxidation and its sequelae in Alzheimer's disease brain contribute to neuronal death. *Neurobiol. Aging* **23**, 655–664.

Cao, G., and Cutler, R. G. (1995). Protein oxidation and aging. I. Difficulties in measuring reactive protein carbonyls in tissues using 2, 4-dinitrophenylhydrazine. *Arch. Biochem. Biophys.* **320**, 106–114.

Cassel, J.-C., Cosquer, B., Galani, R., and Kuster, N. (2004). Whole-body exposure to 2.45 GHz electromagnetic fields does not alter radial-maze performance in rats. *Behav. Brain Res.* **155**, 37–43.

Chaturvedi, C. M., Singh, V. P., Singh, P., Basu, P., Singaravel, M., Shukla, R. K., and Dhavan, A. (2011). 2.45 GHz (CW) microwave irradiation alters circadian organization, spatial memory, DNA structure in the brain cells and blood cell counts of male mice, *Mus musculus*. *Progress in Electromagnetics Res. B* **29**, 23–42.

Choi, H., Park, C. S., Kim, B. G., Cho, J. W., Park, J. B., Bae, Y. S., and Bae, D. S. (2001). Creatine kinase B is a target molecule of reactive oxygen species in cervical cancer. *Mol. Cells* **12**, 412–417.

Cosquer, B., Kuster, N., and Cassel, J.-C. (2005). Whole-body exposure to 2.45 GHz electromagnetic fields does not alter 12-arm radial-maze with reduced access to spatial cues in rats. *Behav. Brain Res.* **161**, 331–334.

Das, K., Samanta, L., and Chainy, G. B. N. (2000). A modified spectrophotometric assay of superoxide dismutase using nitrite formation by superoxide radicals. *Indian J. Biochemi. Biophys.* **37**, 201–204.

Dawe, A., Smith, B., Thomas, D., Greedy, S., Vasic, N., Gregory, A., Loader, B., and de Pomerai, D. (2006). A small temperature rise may contribute towards the apparent induction by microwaves of heat-shock gene expression in the nematode Caenorhabditis elegans. *Bioelectomagnetics* **27**, 88–97.

Fagan, J. M., Sleczka, B. G., and Sohar, I. (1999). Quantitation of oxidative damage to tissue proteins. *Int. J. Biochem. Cell Biol.* **31**, 751–757.

Gandhi, O. P., Hunt, E. L., Andrea. J. A. D. (1977). Deposition of electromagnetic energy in animals and in models of man with and without grounding and reflector effects. *Radio Sci.* **12**(6S), 39–47.

Guimaraes, A. C., and Linden, R. (2004). Programmed cell death. Apoptosis and alternative death styles. *Eur. J. Biochem.* **271**, 1638–1650.

Hara, H., Araya, J., Takasaka, N., Fujii, S., Kojima, J., Yumino, Y., Shimizu, K., Ishikawa, T., Numata, T., Kawaishi, M., *et al.* (2012). Involvement of creatine kinase B in cigarette smoke-induced bronchial epithelial cell senescence. *Am. J. Respir. Cell Mol. Biol.* **46**, 306–312.

Hardell, L., Mild, K. H., and Carlberg, M. (2003). Further aspects on cellular and cordless telephones and brain tumours. *Int. J. Oncol.* **22**, 399–407.

Ikonomidou, C., and Kaindl, A. M. (2011). Neuronal death and oxidative stress in the developing brain. *Antioxid. Redox Signal.* **14**, 1535–1550.

Institute of Electrical and Electronic Engineers (IEEE) (2005). IEEE standard for safety levels with respect to human exposure to radio frequency electromagnetic fields, 3 kHz to 300 GHz. IEEE Topical Review R 282, New York.

Joubert, V., Bourthoumieu, S., Leveque, P., and Yardin, C. (2008). Apoptosis is induced by radiofrequency fields through the caspase-independent mitochondrial pathway in cortical neurons. *Radiat. Res.* **169**, 38–45.

Kaufmann, S. H., Desnoyers, S., Ottaviano, Y., Davidson, N. E., and Poirier, G. G. (1993). Specific proteolytic cleavage of

poly(ADP-ribose) polymerase: An early marker of chemotherapy-induced apoptosis. *Cancer Res*. **53**, 3976–3985.

Lai, H., Horita, A., and Guy, A. (1994). Microwave irradiation affects radial-arm maze performance in the rat. *Bioelectromagnetics* **15**, 95–104.

Laptenko, O., and Prives, C. (2006). Transcriptional regulation by p53: One protein, many possibilities. *Cell Death Differ*. **13**, 951–961.

Lalonde, R. (2002). The neurological basis of spontaneous alternation. *Neurosci. Biobehav. Rev*. **26**, 91–104.

Levine, R. L., Williams, J. R., Stadtman, E. R., and Schacter, E. (1994). Carbonyl assays for determination of oxidatively modified proteins. *Methods Enzymol*. **233**, 346–357.

Li, Z., Yun, P. R., Ming, W. S., Feng, W. L., Bing, G. Y., Ji, D., Xiang, L., and Tao, S. Z. (2012). Relationship between cognition function and hippocampus structure after long-term microwave exposure. *Biomed. Environ. Sci*. **25**, 182–188.

Liu, X., Li, P., Widlak, P., Zou, H., Luo, X., Garrard, W. T., and Wang, X. (1998). The 40-kDa subunit of DNA fragmentation factor induces DNA fragmentation and chromatin condensation during apoptosis. *Proc. Natl. Acad. Sci. U.S.A*. **95**, 8461–8466.

Mantha, S. V., Prasad, M., Kalra, J., and Prasad, K. (1993). Antioxidant enzymes in hypercholesterolemia and effects of vitamin E in rabbits. *Atherosclerosis* **101**, 135–144.

McRee, D. I., and Wachtel, H. (1980). The effects of microwave radiation on the vitality of isolated frog sciatic nerves. *Radiat. Res*. **82**, 536.

Morris, R. (1984). Developments of a water-maze procedure for studying spatial learning in the rat. *J. Neurosci. Methods* **11**, 47–60.

Neves, G., Cooke, S. F., and Bliss, T. V. P. (2008). Synaptic plasticity, memory and the hippocampus: A neural network approach to causality. *Nat. Rev. Neurosci*. **9**, 65–75.

Odaci, E., Bas, O., and Kaplan, S. (2008). Effects of prenatal exposure to a 900 megahertz electromagnetic field on the dentate gyrus of rats: A stereological and histopathological study. *Brain Res*. **1238**, 224–229.

Ohkawa, H., Ohishi, N., and Yagi, K. (1979). Assay for lipid peroxides in animal tissues by thiobarbituric acid reaction. *Anal. Biochem*. **95**, 351–358.

Ozturk, E., Demirbilek, S., Kadir, B. A., Saricicek, V., Gulec, M., Akyol, O., and Ozcan, E. M. (2005). Antioxidant properties of propofol and erythropoietin after closed head injury in rats. *Prog. Neuropsychopharmacol Biol. Psychiatry*. **29**, 922–927.

Riley, T., Sontag, E., Chen, P., and Levine, A. (2008). Transcriptional control of human p53-regulated genes. *Nat. Rev. Mol. Cell. Biol*. **9**, 402–412.

Sakaguchi, K., Herrera, J.E., Saito, S., Miki, T., Bustin, M., Vassilev, A., Anderson, C. W., Appella, E. (1998). DNA damage activates p53 through a phosphorylation–acetylation cascade. *Genes Dev*. **12**, 2831–2841.

Salford, L. G., Brun, A. E., Eberhardt, J. L., Malmgren, L., and Persson, B. R. (2003). Nerve cell damage in mammalian brain after exposure to microwaves from GSM mobile phones. *Environ. Health Perspect*. **111**, 881–883.

Sanders, M. J., Sick, T. J., Perez-Pinzon, M. A., Dietrich, W. D., and Green, E. J. (2000). Chronic failure in the maintenance of long-term potentiation following fluid percussion injury in the rat. *Brain Res*. **861**, 69–76.

Sastry, K. V., Moudgal, R. P., Mohan, J., Tyagi, J. S., and Rao, G. S. (2002). Spectrophotometric determination of serum nitrite and nitrate by Copper. *Anal. Biochem*. **306**, 79–82.

Shahin, S., Mishra, V., Singh, S. P., and Chaturvedi, C. M. (2014). 2.45-GHz microwave irradiation adversely affects reproductive function in male mouse, *Mus musculus* by inducing oxidative and nitrosative stress. *Free Radic. Res*. **48**, 511–525.

Shahin, S., Singh, V. P., Shukla, R. K., Dhawan, A., Gangwar, R. K., Singh, S. P., and Chaturvedi, C. M. (2013). 2.45 GHz microwave irradiation induced oxidative stress affects implantation or pregnancy in mice, *Mus musculus*. *Appl. Biochem. Biotechnol*. **169**, 1727–1751.

Shankaranarayana, R. B. S., and Raju, T. R. (2004). The Golgi techniques for staining neurons. In: *Brain and Behavior* (T. R. Raju, B. M. Kutty, T. N. Sathyaprabha, R. B. S. Shankaranarayana, Eds.), pp. 108–111. NIMHANS, Bangalore.

Suh, J., Rivest, A. J., Nakashiba, T., Tominaga, T., and Tonegawa, S. (2011). Entorhinal cortex layer III input to the hippocampus is crucial for temporal association memory. *Science* **334**, 1415–1420.

Tewari, M., Quan, L. T., O'Rourke, K., Desnoyers, S., Zeng, Z., Beidler, D. R., Poirier, G. G., Salvesen, G. S., and Dixit, V. M. (1995). Yama/CPP32 beta, a mammalian homolog of CED-3, is a CrmA-inhibitable protease that cleaves the death substrate poly(ADP-ribose) polymerase. *Cell* **81**, 801–809.

von Bohlen und Halbach, O., Zacher, C., Gass, P., and Unsicker, K. (2006). Age-related alterations in hippocampal spines and deficiencies in spatial memory in mice. *J. Neurosci. Res*. **83**, 525–531.

Vorhees, C. V., and Williams, M. T. (2006). Morris water maze: Procedures for assessing spatial and related forms of learning and memory. *Nat. Protoc*. **1**, 848–858.

Wallimann, T., Tokarska-Schlattner, M., and Schlattner, U. (2011). The creatine kinase system and pleiotropic effects of creatine. *Amino Acids* **40**, 271–1296.

Wang, B., and Lai, H. (2000). Acute exposure to pulsed 2450-MHz microwaves affects water-maze performance of rats. *Bioelectromagnetics* **21**, 52–56.

Wendt, S., Dedeoglu, A., Speer, O., Wallimann, T., Beal, M. F., and Andreassen, O. A. (2002). Reduced creatine kinase activity in transgenic amyotrophic lateral sclerosis mice. *Free* Radi. Biol. Med. **32**, 920–926.

Xu, S., Ning, W., Xu, Z., Zhou, S., Chiang, H., and Luo, J. (2006). Chronic exposure to GSM 1800-MHz microwaves reduces excitatory synaptic activity in cultured hippocampal neurons. Neurosci. Lett. **398**, 253–257.

Yakymenko, I., Tsybulin, O., Sidorik, E., Henshel, D., Kyrylenko, O., and Kyrylenko, S. (2015). Oxidative mechanisms of biological activity of low intensity radiofrequency radiation. *Electromagn. Biol. Med*. 1–16.

Zhuravliova, E., Barbakadze, T., Zaailishvili, E., Chipashvili, M., Koshoridze, N., and Mikeladze, D. (2009). Social isolation in rats inhibits oxidative metabolism, decreases the content of mitochondrial K-Ras and activates mitochondrial hexokinase. *Behav. Brain Res*. **205**, 377–383.